ANL-20/37

Computational Analysis of Water Film Thickness During Rain Events for Assessing Hydroplaning Risk.
Part 2. Rough Road Surfaces

Nuclear Science and Engineering Division

ANL-20/37

Computational Analysis of Water Film Thickness on Roads During Rain Events for Assessing Hydroplaning Risk.
Part 2. Rough Road Surfaces

prepared by
M.A. Sitek and S.A. Lottes
Nuclear Science and Engineering Division, Argonne National Laboratory

July 2020

Table of Contents

List of Figures

List of Tables

1. Introduction

Hydroplaning occurs when a water film forms on a road during a rain event and vehicles are traveling at a speed that does not provide sufficient time for the tires to push the water film out of the tire path. Under these conditions, the tire loses contact with the road and the driver may lose control over the vehicle.

The present study is a part of a multiyear research effort aimed at gaining a better understanding of the factors that contribute to hydroplaning risk in order to minimize the occurrence of hydroplaning accidents. Three-dimensional computational fluid dynamics (CFD) analysis was used to investigate the water film thickness on multilane roads, one of the key parameters in evaluating hydroplaning risk. In the first part of the study, water films forming on wide roadways, i.e. multilane highways with 2, 4, and 6 lanes per side, were analyzed, with varying cross slope, longitudinal slope, and rainfall rate. Roadways with and without curbs and drainage were included in the analysis. The analysis in the first part was limited to nearly smooth asphalt or concrete surfaces because the maximum roughness height that can be specified in a CFD model using wall functions to determine shear stress at the road surface boundary is one half the thickness of computational cell layer adjacent to the boundary and the need to resolve the vertical velocity distribution in a thin water film requires cell layers that are a fraction of a millimeter thick.

In this part of the study, the analysis was extended to consider the influence of pavement roughness over a range extending up 3.6 mm on the development of water film thickness. Various methods of modeling roughness were investigated and are presented: the roughness height model [1], a meshed-out geometry of the macrotexture of the pavement, and a porous region model. The computational results were analyzed and compared with experimental measurements performed by Gallaway et al. [2], [3], [4].

2. Experimental Analysis of Water Film Thickness on Pavements by Gallaway et al.

Gallaway et al. in their experimental study analyzed water flow on a roadway surface under various conditions. The model used in the study was a 4-foot-wide strip of a two-lane road (24 ft wide) with cross-slope ranging from 0.5% to 8%. Longitudinal slope was not included in the conditions modeled. Nine test surfaces of various types were prepared: rounded siliceous gravel Portland cement concrete, rounded siliceous gravel hot mix asphalt concrete, crushed limestone aggregate hot mix asphalt concrete, and crushed siliceous gravel hot mix asphalt concrete. The average texture depths ranged from 0.003 in (0.076 mm) to 0.164 in (4.2 mm). Rain was modeled by means of channels with nozzles that sprayed water onto the tested surfaces. The rainfall intensities varied from 0.5 in/hr to about 6 in/hr. Water depths were measured using a point gage with a metric scale and vernier giving direct readings accurate to 0.2 mm (0.008 inch). Five measurements were made across the pavement width at each of four measurement locations along the flow path.

Water depth measurements were taken at approximately 6, 12, 18, and 24 ft away from the road crown, and a mean was calculated from five readouts at each location. Water depth below the top of the texture was taken to be negative, and above the top of the texture to be positive. The texture depth of a pavement surface was measured with the putty impression method. In this method, a known volume of silicone putty is formed into a sphere and placed on a pavement surface. Then a metal plate is centered over it and pressed down so it gets into contact with the pavement. The calculation of the mean texture depth is based on the volume per area of the pressed putty.

A set of representative textures tested in the experiment, with varying texture depth and average aggregate size, was chosen as a reference to validate the CFD model. The selected surface types are presented in Table 2-1.

Table 2-1: Surface Types and Conditions Tested in Reference [1]

	Texture depth [mm]	Maximum aggregate size [mm]	Cross slope [ft/ft]	Approximate rainfall intensity [in/hr]
Surface 1	0.9	19	0.5, 1, 2, 3, 4	0.5, 1, 2, 3.5, 5.5
Surface 3	0.08	12.7		
Surface 4	0.5	6.4		
Surface 6	3.6	12.7		

Gallaway et al. collected results from 240 test cases and used them to find a correlation between the water depth and the distance from the road crown, texture depth, rain intensity, and surface slope [3]. The best fit function, referred to as the Gallaway equation, obtained by minimization of the error of prediction, is:

$$f_w = 0.00338\, T_{XD}^{0.11} L_p^{0.43} {R_I}^{0.59} {S_x}^{(-0.42)} - T_{XD} \quad (1)$$

where f_w is water film thickness in inches [in], T_{XD} is the average texture depth in inches [in], L_p is the drainage path length in feet [ft], R_I is the rain intensity in inches per hour [in/hr], and S_x is the cross slope [ft/ft]. The effective water film depth that a vehicle tire experiences depends on the material of the tire and how far the material can deform into the pavement texture. For rigid tires with little deformation at the scale of the texture, the water film thickness experienced by the tire is given by the Gallaway equation.

As noted in [3], a decrease in slope results in an increase of the water depth, and the rate of increase is higher for flatter slopes. Also, an increase in texture depth results in a decrease of the water depth, f_w, above the texture. In turn, water depth increases with an increase the drainage area and rainfall intensity.

The experimental findings and the correlation for the water film thickness proposed by Gallaway, et al. were used as a reference in validation process of the CFD modeling.

3. Physics Modeling

The geometry of multilane highways with 2, 4, and 6 lanes per side, was modelled in the STAR-CCM+ CFD software. Lanes are taken to be 12 feet wide. The crown or highpoint is assumed to be the left side of the leftmost lane with rainwater draining across all of the lanes to the right. The models represent a thin strip of the roadway across the travel lanes. The primary geometric parameters are road width, and cross slope. In this part of the study the longitudinal slope was not accounted for. Rainfall rate was also varied in the simulations.

Another significant geometry variation for multilane highways and roads with many lanes is whether or not the roadside is open so that water flowing down the cross slope can freely flow off the roadside or the roadside is curbed with drain grates. The previous part of the study [5] revealed that as long the rainfall intensity and geometry of the road are the same, the water film thickness distribution is the same for a road with or without a curb up to the position where a pool may exist next to the curb. Therefore, only the case of a road with a shoulder, that allows for the water to drain off of the pavement, was modeled.

The water film thickness grows over the cross-street slope from zero or slightly less when the texture depth is subtracted at the high elevation (crown or center divider) to a maximum very near the low elevation of the roadside. Two parameters are of interest: (1) the maximum water film thickness and (2) the fraction of roadway where the water film thickness exceeds a specified value considered to be high risk for hydroplaning. Result analysis sought to identify functional relationships between these measures of water film thickness and the case parameters for a steady state condition where the rain is constant over some time.

4. CFD Modeling

The Unsteady Reynolds Averaged Navier-Stokes Solver with k-epsilon turbulence model was used in the modeling. The Eulerian two-phase model with a gas phase – air, and liquid phase – water, combined with the Volume of Fluid (VOF) physics model was selected to model the water surface. The goal of this study is to model water films on multilane-wide pavements with thickness of a few millimeters order of magnitude. To accurately resolve the interface between air and water, the mesh needs to be significantly denser in the vertical direction than in either of the in-plane directions. Taking these requirements into account, a standard discretization of the volume consisted of a 0.1 mm volume cell size in the vertical direction and a 5 mm size in the horizontal directions. To decrease the computational expense, it was assumed that the longitudinal grade of the road is zero. Assuming spatial and temporal uniformity of the rain on a very long road with constant cross-sectional slopes, a repetitive flow pattern forms along the road and the conditions become almost identical in each section of the road. This assumption made it possible to model the flow with a CFD domain that represents only a thin strip of volume in the direction along the road that extends a much longer length over the cross-slope direction of a road.

Figure 4-1 shows sketches of the type of roadway that was modeled, with the main elements of the road highlighted in the figure, along with the CFD domain with the boundary conditions used for computations. It illustrates a model of a multilane-wide road without a curb, where the water

freely drains off to the side of the road (to the right side). The left side of the domain represents the highest point on the road cross-section, the crown. In the CFD model, the left side surface is modeled as a symmetry boundary condition because no water enters the domain through that boundary and gravity ensures that no water leaves through that boundary, the right-side surface is modeled as a pressure outlet boundary, with backpressure, and the top surface of the domain is modeled as a pressure outlet boundary condition with an atmospheric pressure assigned. The top boundary is sufficiently above the water surface so water never leaves the domain through the top boundary, but air may leave the domain through the top to accommodate a growing water film thickness. The bottom surface of the model is the road surface. Depending on the type of modeling used, the bottom surface was represented in different ways. Details of the pavement surface modeling are given in Section 5. The two surfaces parallel to the page are assigned a symmetry boundary condition because there is no flow in the direction along the street.

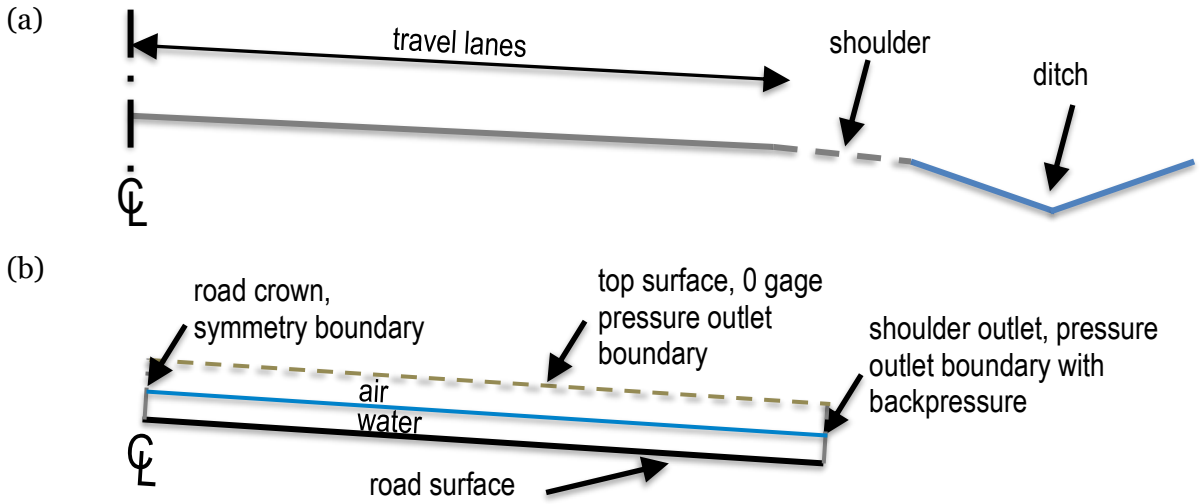

Figure 4-1: Model of a road without a curb: (a) a sketch of a cross-section of a road, (b) a sketch of a CFD domain

Rainwater entering the system is modeled as a volumetric source term in the conservation of mass equation in a small volume right above the road surface. This avoids the computationally expensive modeling of rain entering the water film from above using an additional dispersed phase, multiphase model for the rain drops. Since the net effect of rain falling onto the water film is to increase the water mass flow where the rain droplets hit and join the film, modeling the addition of water mass from rain hitting the film using a mass source term in the differential equations saves a considerable amount of computer resources and run time. This way of modeling rain was presented in the previous technical report [5].

5. Modeling Roughness

The models described and analyzed in the previous part of the study [5] did not account for roughness of the pavement surface greater than 0.15 mm. The road surface was assumed to be nearly smooth due to limits on the maximum roughness height that could be specified for the

required vertical mesh density. This assumption is appropriate for concrete roads and other smooth surfaces including some asphalt, but may not be sufficient for the range of textures of asphalt roads and similar road surfaces, which are usually significantly rougher than concrete. Alternative methods for accounting for the roughness of asphalt roads were investigated, and the methods and results are presented in this section. Roughness of the pavement surface was represented in this study in three ways:

- roughness coefficient or roughness height presented in Section 5.1,
- meshed-out geometry of the surface presented in Section 5.2
- porous region presented in Section 5.3.

The following sections present and discuss the CFD modeling methods and analysis results for these alternative representations of surface roughness.

5.1. Modeling Roughness with a Roughness Coefficient or Height

In hydraulic engineering, the Manning roughness coefficient is often used to characterize roughness, and its values are derived from experiment or assumed from empirical tables. In most CFD software, STAR-CCM+ included, the user needs to specify a roughness height parameter, k_s, giving the equivalent sand-grain roughness height on a surface. Roughness height and Manning's roughness coefficient do not represent the same physical parameter and have different units (k_s has units of length and Manning's n has units of time/length$^{1/3}$). Nevertheless, they both characterize the effect of surface roughness on flow and relations between them have been developed to allow determination of equivalent roughness height in CFD analysis from a given Manning coefficient value. One of these relations is Strickler's equation [6]:

$$n = 0.038\, k_s^{1/6}, \text{ or } \quad k_s = \left(\frac{n}{0.038}\right)^6 \tag{2}$$

where k_s is roughness height and n is the Manning coefficient and the units of k_s are meters.

An alternative relationship between the Manning's roughness coefficient and roughness height can be derived from the rough turbulent portion of the Colebrook-White relation for k_s [6]:

$$\frac{1}{\sqrt{f}} = -2.03\, \log\left(\frac{k_s}{12.27}\right), \tag{3}$$

where f is the Darcy friction factor:

$$f = \frac{8\tau}{\rho V^2}, \tag{4}$$

Assuming a wide stream with hydraulic radius, $R_h = D_h/4$ (hydraulic diameter D_h) approximately equal to the flow depth, d, and combining with the Manning equation gives the friction factor as a function of the Manning number, flow depth, and acceleration of gravity:

$$f = \frac{8gn^2}{d^{\frac{1}{3}}}, \tag{5}$$

Combining this with the Colebrook-White relation, equation (3), yields the roughness height as a function of flow depth, d [m], and the Manning number, n [s/m$^{1/3}$]:

$$k_s = 12.27\, d \left(10^{\frac{d^{(1/6)}}{(-2.03)n\sqrt{8g}}} \right), \tag{6}$$

The use of a mean flow depth is assumed to be adequate for engineering purposes. In CFD computations a local value of roughness height, k_s, that varies with water depth over the domain and has several Manning roughness values for different surfaces can be programmed using equation (6).

Figure 5-1 presents the Strickler and Colebrook-White equivalent roughness height as a function of Manning's coefficient in the range of values corresponding to pavement surfaces, water film depths, and near curb pool depths. McGahey [6] notes that the Strickler relation is only valid for water depths that are 7 to 140 times the roughness height, and that large Manning n values characterizing grass, for example, tend to yield inflated k_s values. The depth constraint means that Strickler's relation is not applicable to water films where the water depth is close to the roughness height. It does apply in a pool region near a curb. In that zone for asphalt with Manning number of 0.016 and a water depth of 60 mm, Strickler's relation gives k_s = 5.6 mm, while McGahey's relation gives k_s = 4.9 mm. At lower water depths, McGahey's relation, which accounts for water depth, gives lower effective roughness heights, and consequently it may provide a better representation of the effective roughness height.

At the length scale of interest for water films on the street during rain events, ranging up to about 6 mm, the effective roughness height may be a significant fraction of the water depth. In CFD analysis, the water film is represented in a grid of cells with 20 to 30 or more cells in the vertical direction. The effective roughness height is limited to one half the height of the layer of computational cells adjacent to the road surface, beyond that it has no effect. As noted in Section 4, the height of cell layers or the analysis is about 0.1 mm, limiting the roughness height to about 0.05 mm, far smaller than the range of roughness of road surfaces that may be up to about 3.6 mm, Table 2-1. As a consequence, the modeling of roughness in the flow of the water film beyond nearly a nearly smooth road surface requires alternative approach. The following sections present investigations and results of modeling roughness by simply meshing out the roughness explicitly, which is computationally expensive, and by using a porous media model to characterize the rough layer.

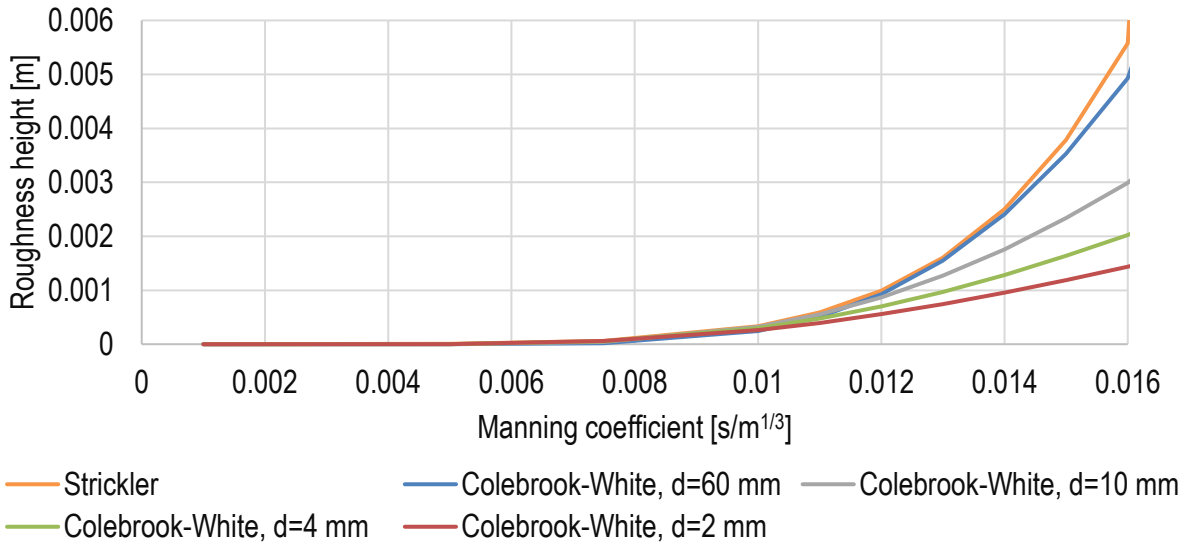

Figure 5-1: Prediction of roughness height from Manning coefficient by Colebrook-White and Strickler formulas

5.2. Modeling Roughness with the Meshed-Out Geometry Model

The most obvious way to capture the effects of significant roughness at the road surface (e.g. asphalt), when the water film height is at most a few times the roughness height, is to mesh out the roughness of the surface.

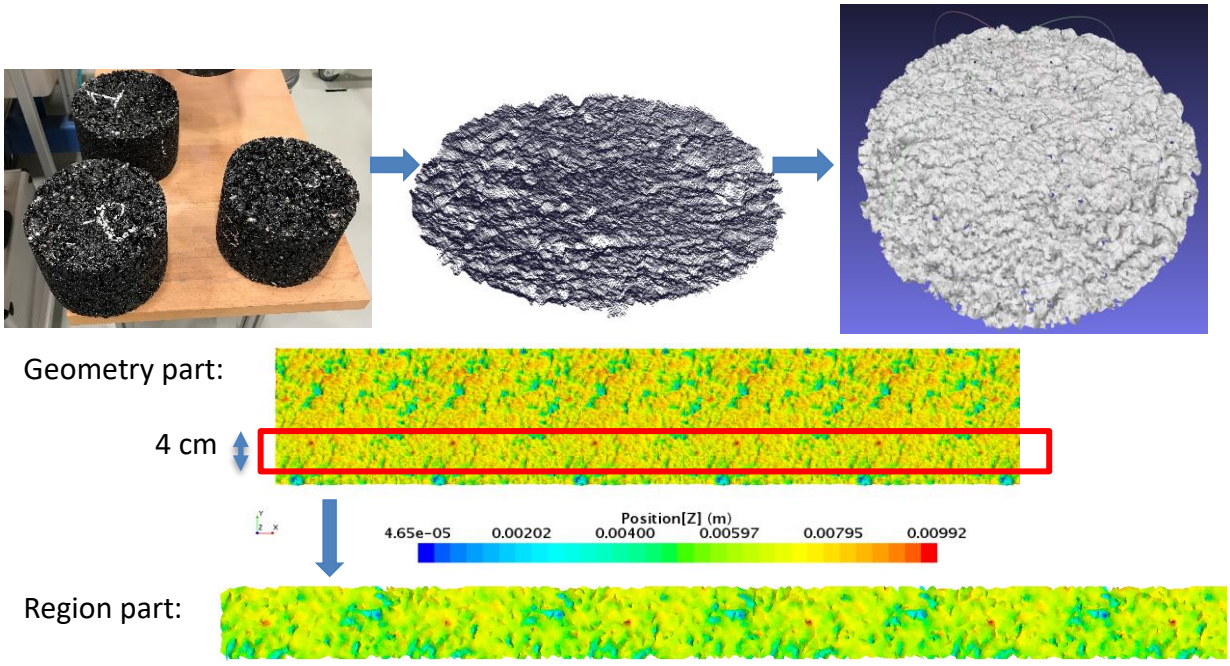

Figure 5-2: Workflow for preparing a rough surface for CFD simulation

In this study, Argonne researchers obtained a point cloud from a laser scan of a pavement sample from the Turner-Fairbank Highway Research Center. The data was transformed into a stereolithographic (STL) file and a square piece was cut out from the circular surface. The square section, 0.1 m by 0.1 m, of pavement texture was stitched together to create a long strip. This strip was used as a pavement surface in the geometry of a CFD model and a wall boundary condition was assigned to it. To conserve computational resources and reduce run times, the strip width was reduced from 10 cm 4 cm. The 4 cm width was assumed to be sufficient to provide a 3D characterization of the street surface in the longitudinal direction, while a longer 3.6 m length was needed to characterize the 3D flow development in the cross-street direction. The cross-street direction is the primary flow direction for drainage when the longitudinal slope is much smaller that the cross slope, and in these cases the longitudinal slope was zero. The workflow is presented in Figure 5-2.

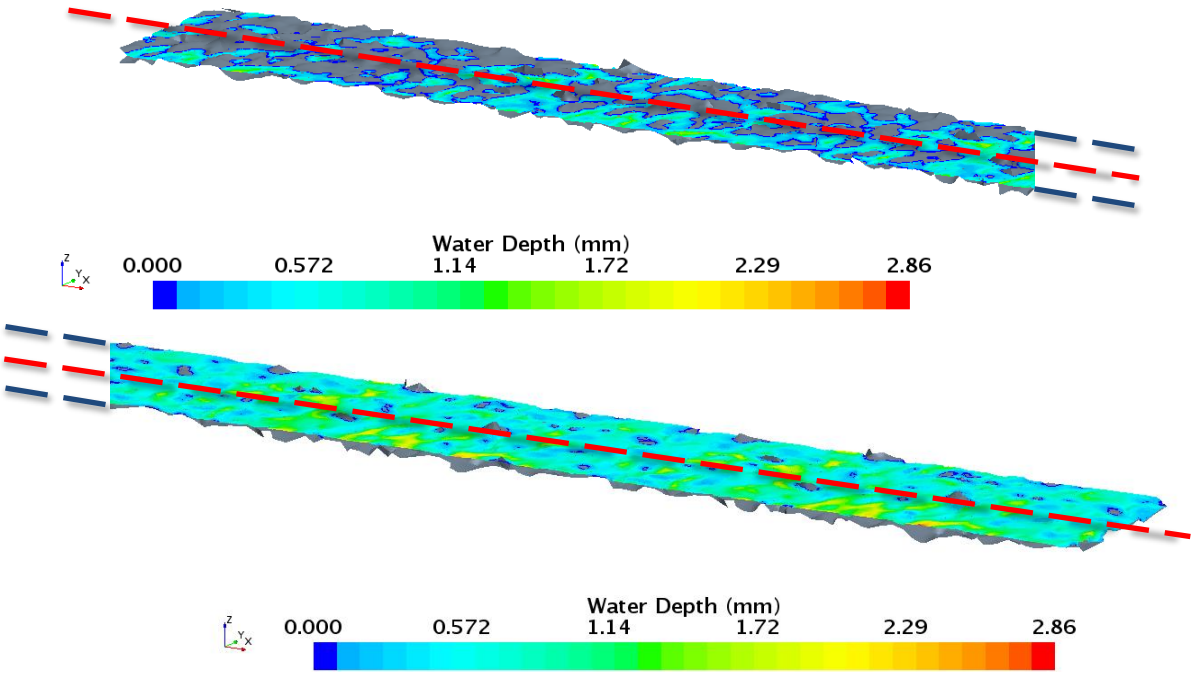

Figure 5-3: Water depth on a rough pavement, (a) close to the median, (b) close to the shoulder. Rainfall intensity 2 in/hr, slope 2%.

The resulting road surface geometry has multiple very small asperities, some a fraction of a millimeter in size. Such small detail is not currently feasible to represent in the computational domain, because it would result in tens to hundreds of millions of computational cells in even a relatively small problem, and thus would be too computationally expensive to solve with currently available computational resources. Consequently, the surface was smoothed out during the meshing process, with a 2 mm base cell size in the horizontal directions. Two models were developed, a 1-lane and a 2-lane strip of road with a 2% cross slope. The first one resulted in a ~4 million cell model, and the latter in an ~11 million cell model. The rainfall intensity was varied from 2 in/hr to 10 in/hr.

The meshed out rough surface model makes it possible to observe and analyze the flow in greater detail than possible with a smooth flat surface model. Figure 5-3 shows a contour plot of water depth on two ends of the strip: at the median and at the shoulder. The road surface was plotted in grey in the figures. Close to the median, there are patches with no water, or the water is contained in small depressions with surface level lower than the asperities. Far from the median, the water depth is higher, and covers almost all asperities. The water surface is not flat, as ripples form due to the roughness of the pavement.

Calculating the water depth relevant to the hydroplaning analysis is challenging because of the variation in surface height and the small size of the irregularities in the geometry. A tire on a moving vehicle does not come in contact with the entire surface of the road, but only with the top portion of the surface because it is not flexible enough to conform to the small depressions. To calculate the water film thickness in this study, a simplification of the surface is proposed. Figure 5-4 shows surface height on a line going through the center of the road strip model (blue solid line) and two iterations of smoothing (first – dark blue solid line, second-green dashed line), which was done by connecting the neighboring local maxima.

Figure 5-5 presents the road and water surface on a centerline at 2 ft to 4 ft from the median for rainfall intensity 2 in/hr. The results for a portion of the road far downstream from the median are shown in Figure 5-6. Figure 5-7 shows a comparison of water film thickness prediction by various models: a rough surface model, smooth surface models and the Gallaway equation [4]. The water film thickness for the rough surface model was calculated by subtraction of the second iteration of smoothing from the water level height. Close to the median, the smooth surface solution gives a nonzero water depth, whereas the rough surface solution has patches of zero water depth. Far from the median, the smooth surface solution again gives values higher than the average rough surface solution. The Gallaway et al. equation gave negative water film thickness up to 6.5 ft away from the median. Far away from the median the thickness is in good agreement with the rough surface solution.

The simulation was also run with higher values of rainfall intensity, 5 in/hr and 10 in/hr. The results are depicted in figures from Figure 5-8 to Figure 5-11. Near the median, the smooth surface solution always exceeds the rough surface solution, because the zero for water film depth is at the top of the asperities, and at the median the water builds up from the bottom of the asperities. Roughness decreases flow velocity compared to a smooth surface and given enough flow length the water film thickness for rough surfaces will overtake and exceed that of the smooth solution because total flow cross section area is bigger to accommodate the slower flow at the same discharge. The distance to the cross over point decreases as rain intensity increases.

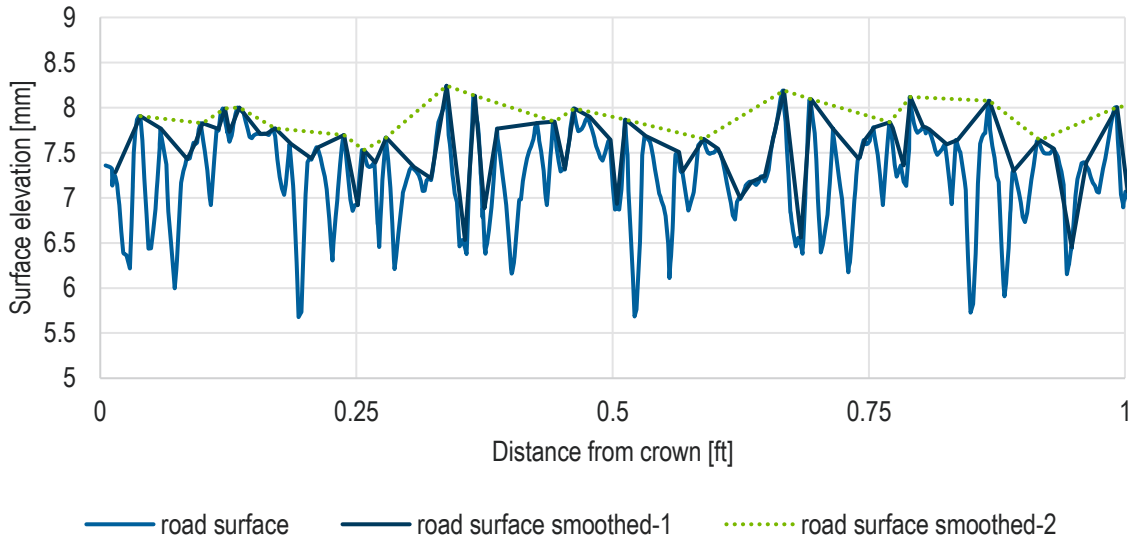

Figure 5-4: Road surface on a centerline from the crown to 1 ft from the crown

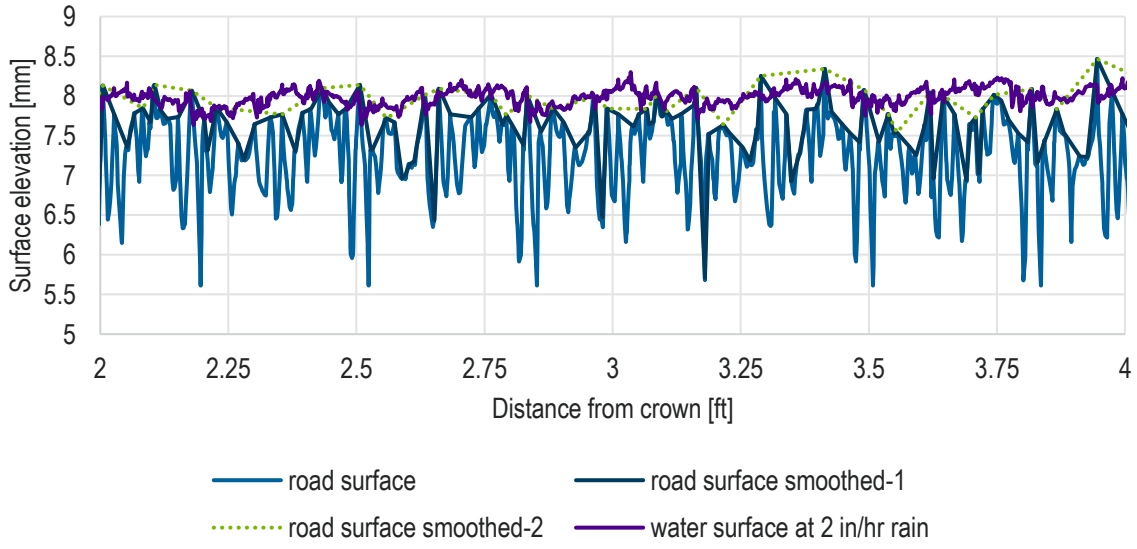

Figure 5-5: Road and water surface on a centerline at 2 ft to 4 ft from the crown. Rainfall intensity 2 in/hr, cross slope 2%.

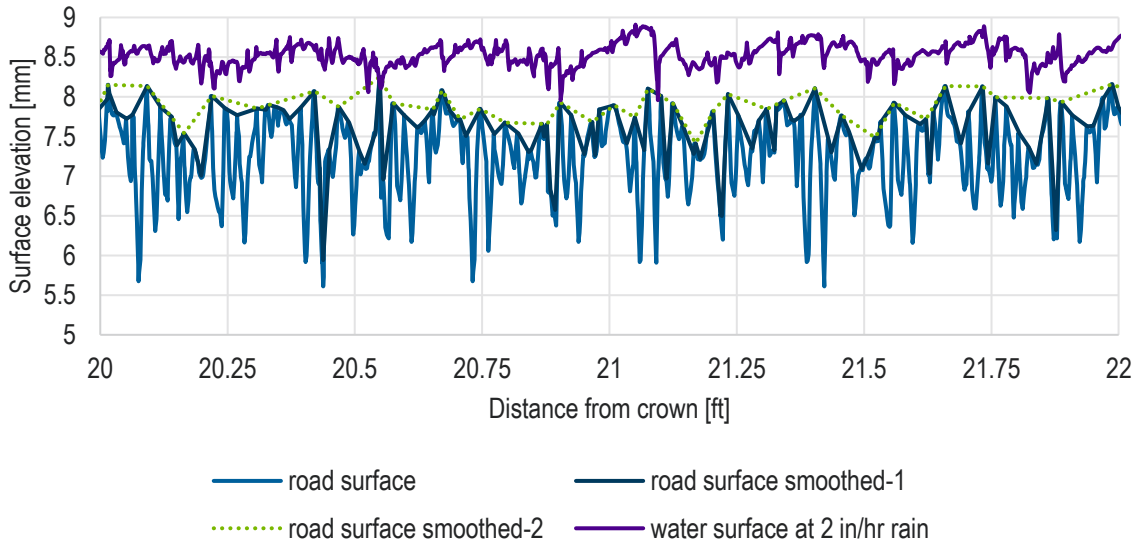

Figure 5-6: Road and water surface on a centerline at 20 ft to 22 ft from the crown. Rainfall intensity 2 in/hr, cross slope 2%.

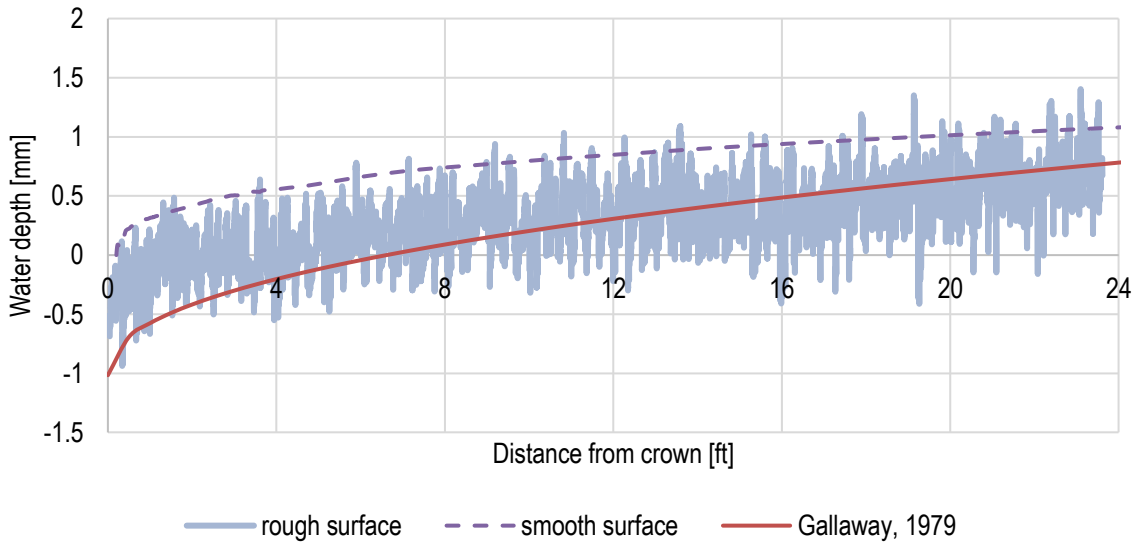

Figure 5-7: A comparison of the water film thickness prediction by the rough surface model, smooth surface models: without and with curb, and Gallaway equation for a 2 in/hr rain

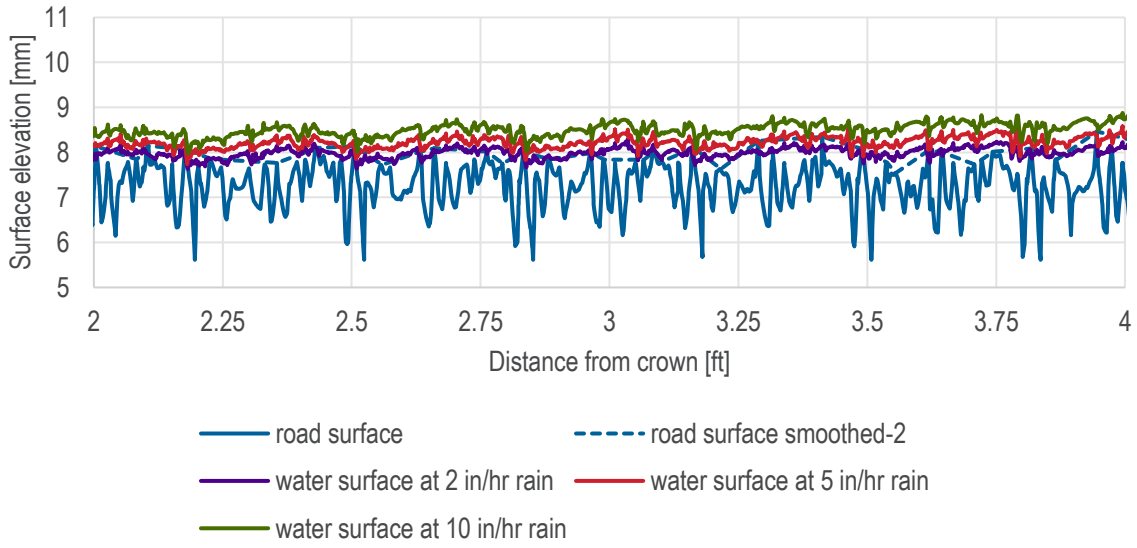

Figure 5-8: Road and water surface on a centerline at 2 ft to 4 ft from the median. Rainfall intensity: 2 in/hr, 5 in/hr, 10 in/hr, cross slope 2%.

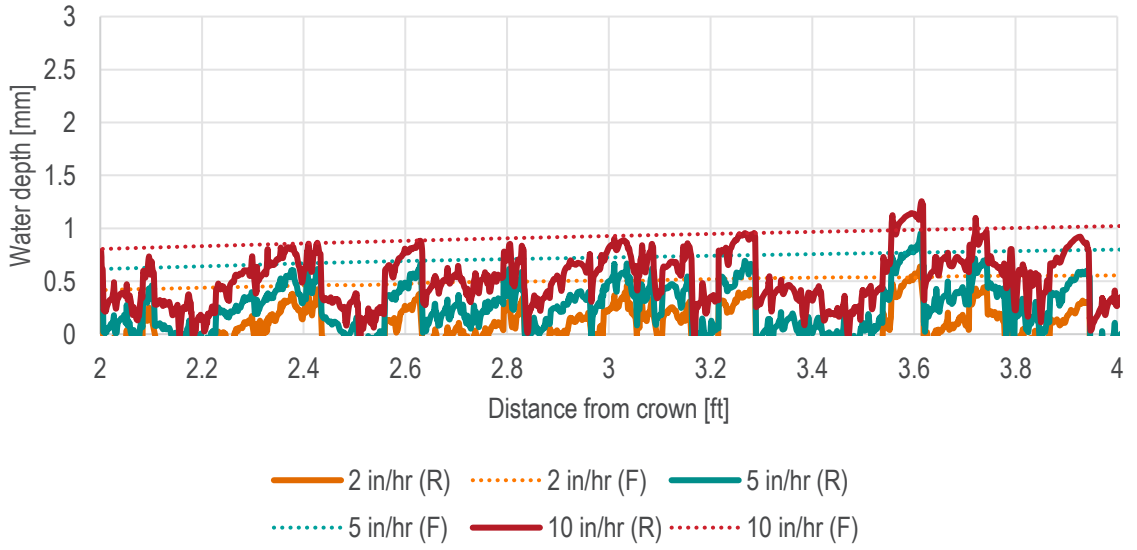

Figure 5-9: Water depth on a centerline obtained from CFD simulations using a smooth flat surface (F) and a rough surface (R) at 2 ft to 4 ft from the median. Rainfall intensity: 2 in/hr, 5 in/hr, 10 in/hr, slope 2%.

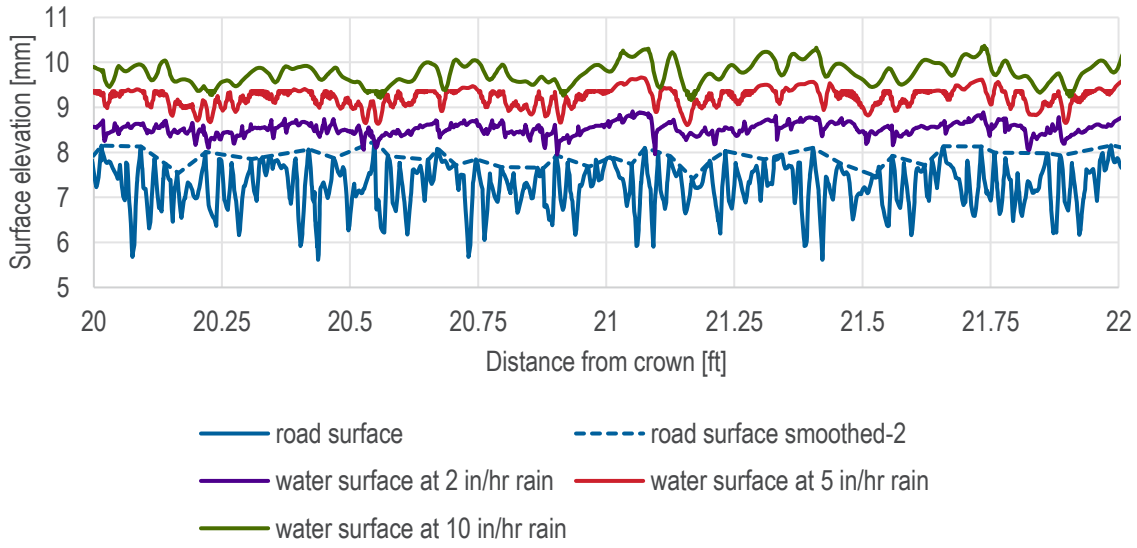

Figure 5-10: Road a water surface at 20 ft to 22 ft from the median. Rainfall intensity: 2 in/hr, 5 in/hr, 10 in/hr, slope 2%.

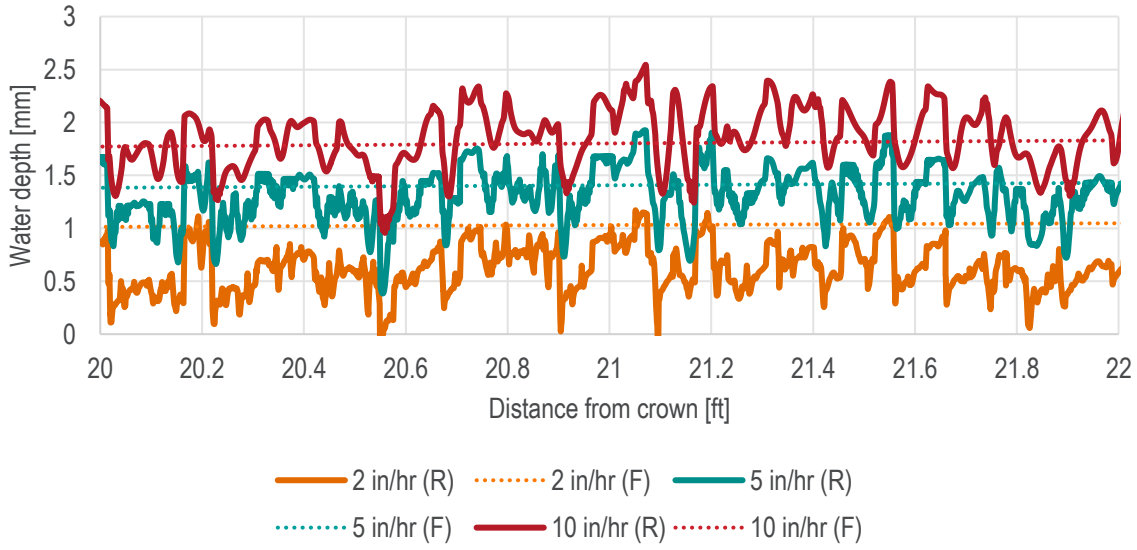

Figure 5-11: Water depth obtained from CFD simulations using a smooth flat surface (F) and a rough surface (R) at 20 ft to 22 ft from the median. Rainfall intensity: 2 in/hr, 5 in/hr, 10 in/hr, slope 2%.

A different variant of surface roughness, a surface with grooves across the roadway, was modeled in the CFD software. The asperities are approximately 6 mm high, with maximum height of 7.7 mm. Two cross sections were chosen for monitoring of the water depth, one crossing through the tops of the asperities, and another one going through the lowest part of the surface. Again, three rainfall intensities were selected, 2 in/hr, 5 in/hr, and 10 in/hr. The road strip has a cross slope of

2%. A top view of a section of the roadway surface model with a contour plot of the vertical coordinate is presented in Figure 5-12. The cross-sections, plane sections 1 and 2, are marked in red in the figure. Figure 5-13 shows a plot of the road surface Z coordinate along the red lines at a distance of one foot from the crown.

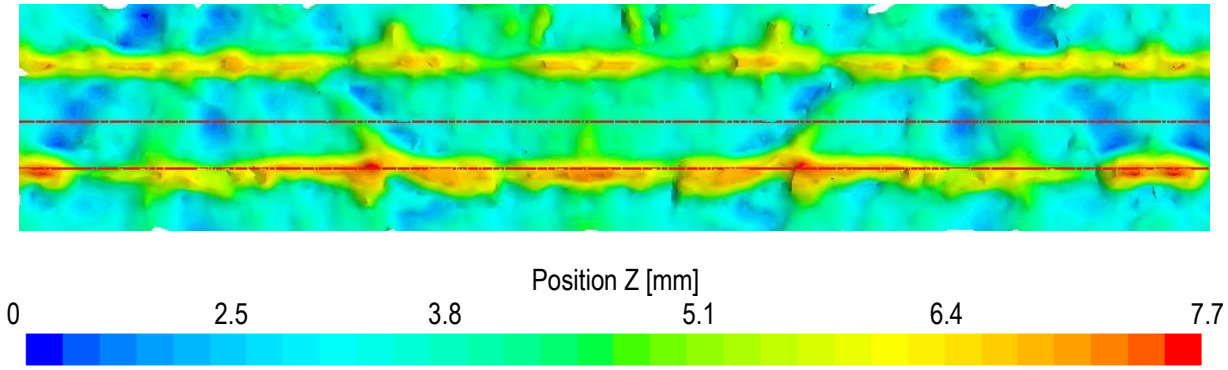

Figure 5-12: Top view of a section of the roadway surface model with a contour plot of vertical coordinate. Plane sections 1 and 2 are marked in red.

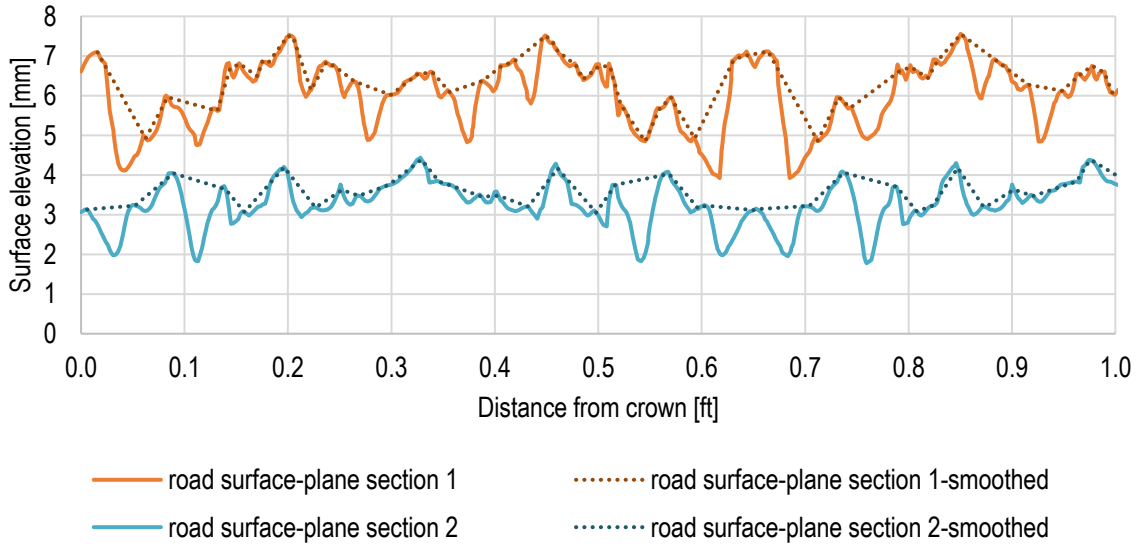

Figure 5-13: Road surface on plane sections 1 and 2 between the 0 ft to 1 ft from the median

The plane section 1 goes through the peaks of the road surface; therefore, the water film thickness is significantly lower than along plane section 2. At rainfall intensity 2 in/hr, the water level falls below the height of the asperities. The water depth was calculated in two ways. Firstly, by subtracting the Z coordinates of a smoothed road surface (calculated as in the previous example) from Z coordinates of the water surface, and secondly, by subtracting an average road surface height. Also, a moving average of the two curves was calculated to reduce the fluctuations. The two approaches give similar results with a difference in average values ranging from a fraction of a millimeter up to 0.3 mm of water depth. Figure 5-14 shows the water depth plots along plane section 2 for rain intensity 2 in/hr. Figure 5-15 and Figure 5-16 present results for a 5 in/hr rain,

and Figure 5-17 and Figure 5-18 for a 10 in/hr rain. There is an increase in the water film thickness, as well as the portion of the surface covered with water, due to the higher rainfall intensities.

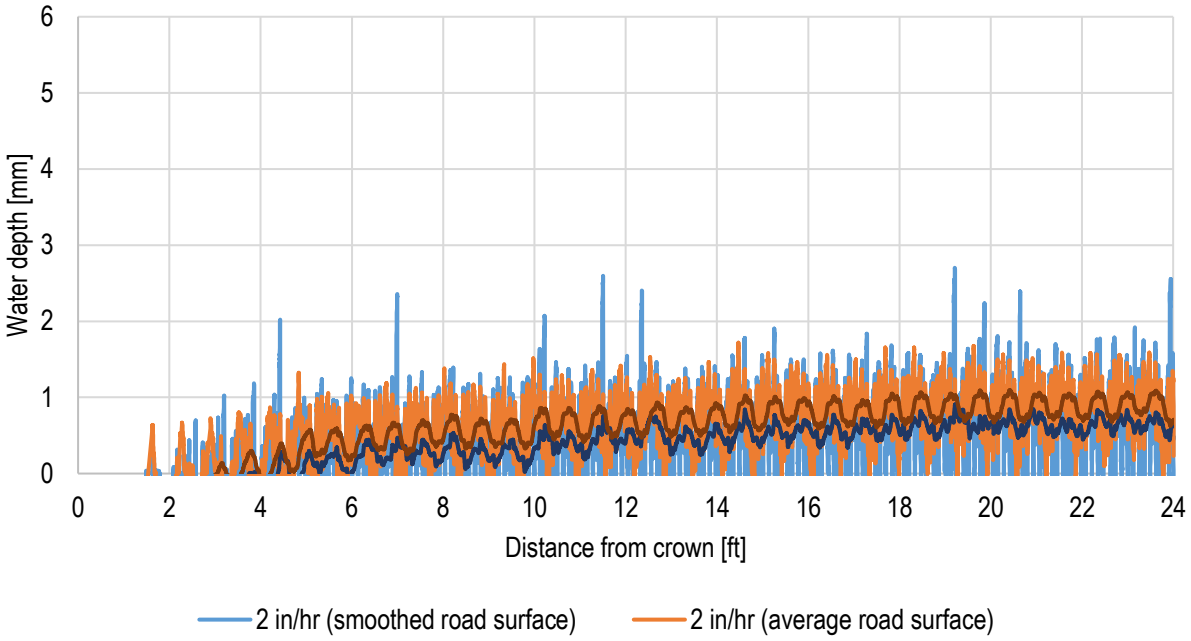

Figure 5-14: Water depth on a cross section (plane section 2) at 2 in/hr

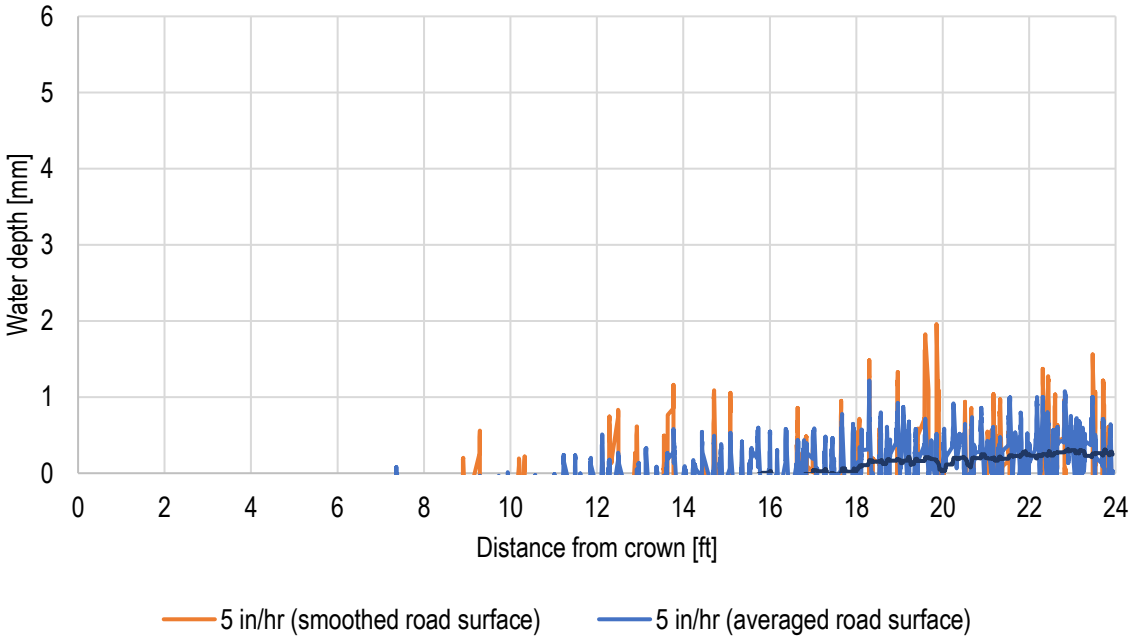

Figure 5-15: Water depth on a cross section (plane section 1) at 5 in/hr

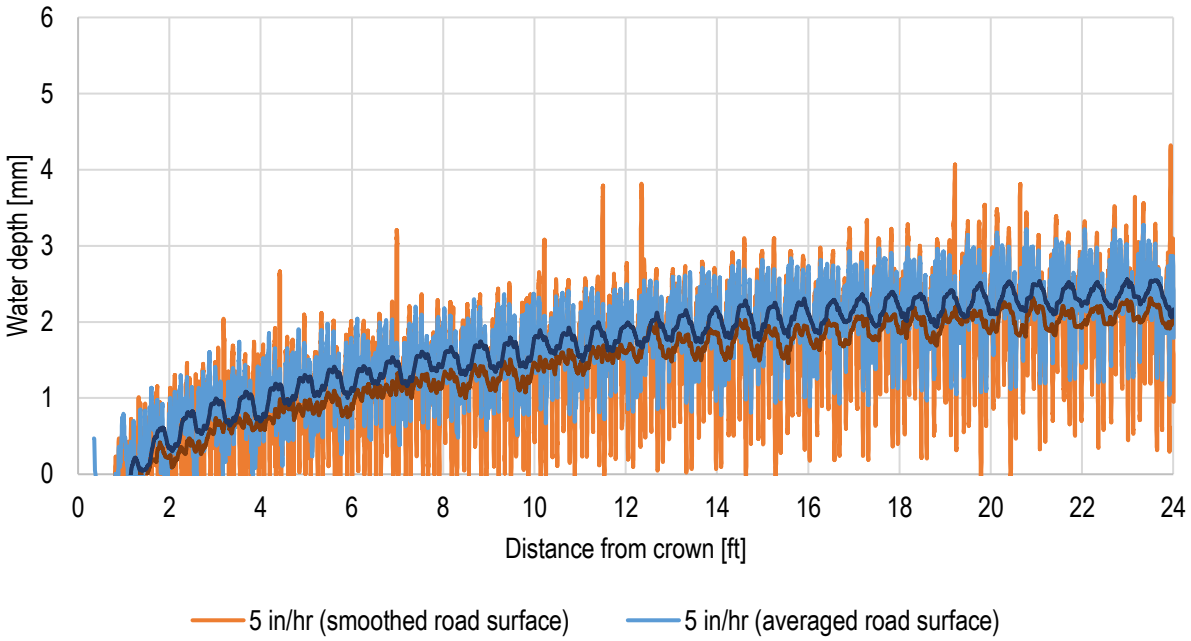

Figure 5-16: Water depth on a cross section (plane section 2) at 5 in/hr

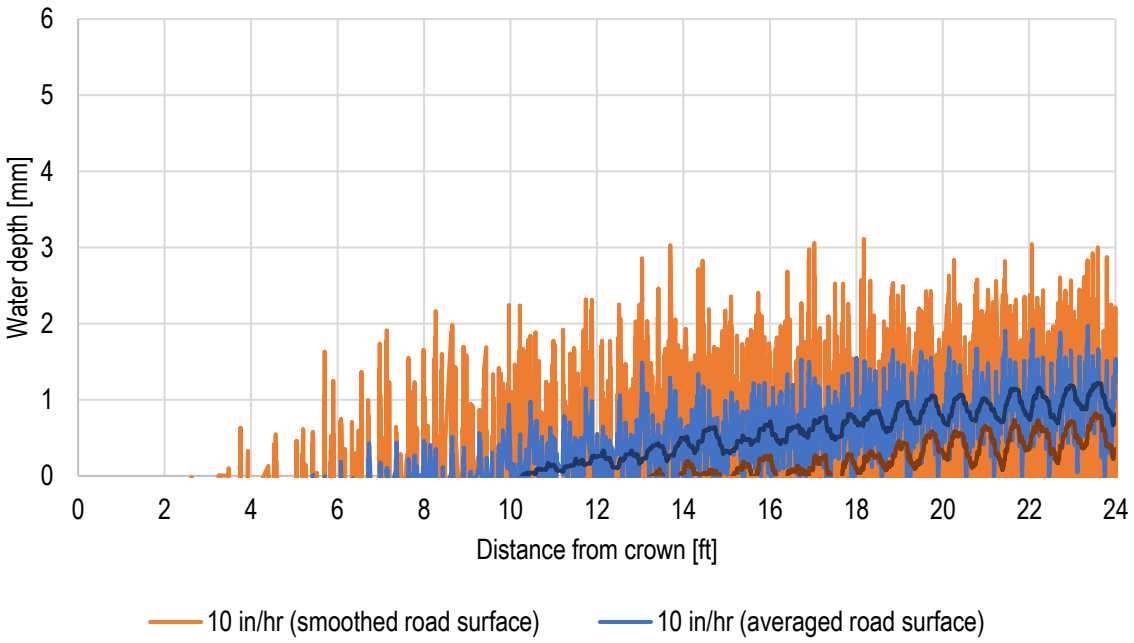

Figure 5-17: Water depth on a cross section (plane section 1) at 10 in/hr

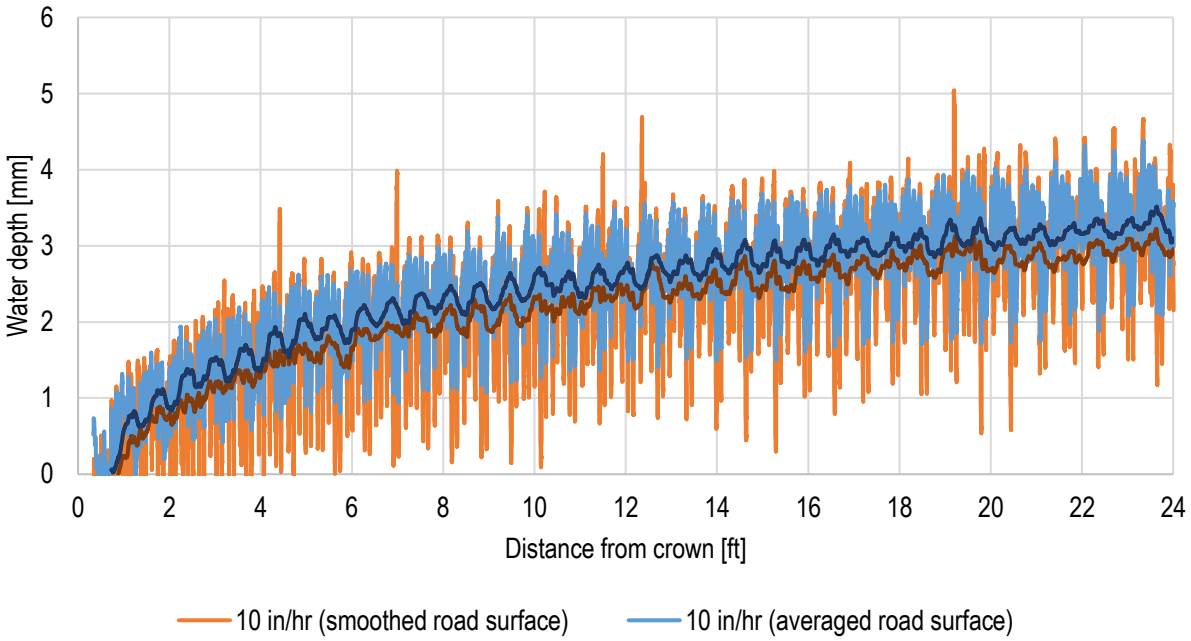

Figure 5-18: Water depth on a cross section (plane section 2) at 10 in/hr

5.3. Modeling Roughness as a Porous Region

The third approach to modeling roughness assumes that the pavement surface is approximated with a bed of spherical particles that represents the aggregate.

In the Gallaway experiments, the mean texture depth of the pavement surfaces was measured with the putty impression method. In this method, a known volume, V_p , of silicone putty is formed into a sphere and placed on a pavement surface. Then a metal plate with circular depression of thickness t_0 is centered over it and pressed down until the raised surface of the plate comes into contact with the top of the macro texture on the pavement. A circular patch of putty with diameter D results. The sum of the volumes of putty above, V_d, and below, V_T, the surface texture must equal the known volume of putty,

$$V_p = V_d + V_T \tag{7}$$

Define the texture depth, T_{XD}, as the texture void volume, V_T, per unit projected area, which is the putty patch area, $A_p = \pi D^2/4$:

$$T_{XD} = \frac{V_T}{A_p} = \frac{V_p - V_d}{A_p}, \tag{8}$$

Let $d_0$be the diameter of the patch of putty when the surface is perfectly smooth, then the volumes are:

$$V_p = \frac{\pi d_0^2 t_0}{4},\ V_d = \frac{\pi D^2 t_0}{4},\ V_T = \frac{\pi D^2 T_{XD}}{4}, \tag{9}$$

combining with Equation 7 gives:

$$T_{XD} = \frac{d_0^2 t_0}{D^2} - t_0, \tag{10}$$

Gallaway [2] used a plate with a 1/16 inch depression, t_0, and an amount of putty that compressed to a 4 inch diameter circle on a smooth surface, d_0. In this case Equation 10 reduced to

$$T_{XD} = \frac{1}{D^2} - t_0, \tag{11}$$

where D, t_o, and T_{XD}, are in inches. To determine T_{XD} for a surface texture, the putty was compressed four times into the surface texture and the average of the putty patch was calculated to determine D.

In a porous media model of the road macro texture, the porous layer must have sufficient volume for both the void space and the solids. This requirement leads to a relation between the roughness height or thickness of the porous layer, k_s , the porosity, χ, defined as the ratio of open volume to the total volume, the texture depth, T_{XD}, and projected area, A_p,

$$V_T = \chi\, k_s\, A_p. \tag{12}$$

Therefore, the thickness of the porous layer is:

$$k_s = \frac{T_{XD}}{\chi}. \tag{13}$$

To illustrate in a clear example that is not a real road texture, if the texture consists of a set of square cross section channels alternating with equal square cross section solid texture as in Figure 5-19, then half the volume is void and half solid texture, giving a porosity of 0.5 and a porous layer thickness and roughness height of $k_s = 2\, T_{XD}$.

Figure 5-19: Simplified illustration of porous layer surface texture where the texture occupies half the volume void space is half the volume

The rough pavement surface was modeled as a packed bed of spheres with diameter equal to the maximum aggregate size and thickness of the roughness height, k_s, calculated from Equation 12 and the mean texture depth, T_{XD}, (listed in Table 2-1). A porous medium is characterized by three parameters: porosity, porous inertial resistance, and porous viscous resistance. The resistance to flow within the porous media is related to the surface area per unit volume, which is determined from the aggregate size and porosity, χ. Higher porosities lead to lower flow resistance and vice versa. Because the Gallaway surface data do not include porosity or information from which it can

be calculated, three values of porosity, 0.3, 0.5, and 0.7 were tested using the model to determine water film thickness and compared to the experimental measurements to identify the porosity value that best fits the experimental data. The porosity value for the various textures in Gallaway's experiments may have varied, and if more accurate results are desired, then additional research may be performed to determine porosities for the textures in different types of pavements.

The porous resistance was estimated from the Ergun relationship between pressure drop across a length of a porous region and fluid velocity for a packed bed of spheres [1]:

$$-\frac{\mathrm{d}p}{L} = P_v v_s + P_i, v_s^2,$$
$$P_v = \frac{150\mu(1-\chi)^2}{\chi^3 D_p^2},\ P_i = \frac{1.75\rho(1-\chi)}{\chi^3 D_p} \tag{14}$$

where P_v is the viscous term, P_i is the inertial term, ρ is fluid density, μ is fluid dynamic viscosity, v_s is fluid superficial velocity through the medium, and D_p is particle diameter (aggregate size). From Equation 14, decreasing the aggregate size increases the porous resistance because the aggregate surface area per unit volume increases, and it is the zero velocity boundary condition at the surface that creates the resistance. If the aggregate size covers a range of values, then using the smallest aggregate size may capture the aggregate surface to volume ratio reasonably well and err on the conservative side making the porous resistance values slightly larger than in reality.

The bottom surface of the domain is a no-slip wall boundary. In the porous media model, the details of flow in the void space are not calculated and the flow solution represents a volume average that accounts for the presence of the surface texture without resolving the asperities in the surface. A sketch of a CFD two-region model is presented in Figure 5-20. The bottom region is a porous media region, and the region on top is a fluid region. An internal interface is created between the regions.

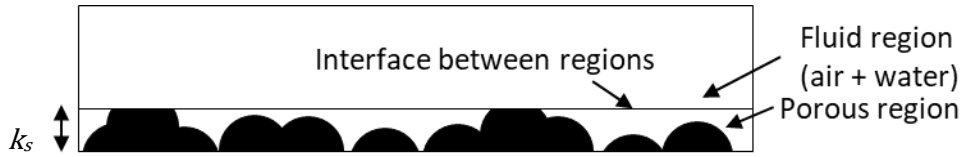

Figure 5-20: Example of a surface profile and its representation with a porous medium

The Gallaway et al. report [3] provides a variety of useful information about the setup of the experiments, water depth measurements for varying road and rain conditions, as well as an analysis of the results. Nevertheless, to develop an accurate CFD model of the tests, more details are needed. Only the maximum aggregate size was provided for each surface, whereas a size distribution would give more insight into the porous characteristics of the surface, and the smallest aggregate size is probably the best to use for calculating the porous resistances. Also, the macrotexture depth was given as the mean texture depth, T_{XD}, with no information regarding the porosity of the texture. In the present times, a scan of the macrotexture, such as presented in Chapter 5.2, would allow calculation of porosity and texture depth.

The CFD analysis was performed with a rough pavement porous region having porosities of 30%, 50%, and 70%, as well as modeled as a smooth surface, thus making it possible to establish which porosity value is the most suitable for the problem, and to determine the range of texture depths in which assuming a smooth surface in the CFD model may be good enough for engineering application.

Figure 5-21 shows the distribution of water depth along a cross-section of road with mean texture depth 0.5 mm, cross-slope 0.5%, and rain intensity 2.21 in/hr. In the experiment, all measurements had positive values, which means that the water depth exceeded the mean texture depth and that a tire can come in contact with the water film. The computational results for the rough surface models and a smooth surface model are compared with the experimental data points and a curve obtained from the Gallaway equation. The rough surface model with 30% porosity is a close match to the Gallaway equation prediction. Both overestimate the experimental measurements. The model with 50% porosity goes through the points, and the model with 70% porosity underestimates the experimental results by a small amount. The smooth surface CFD model result falls in between the experimental data points, close to the 50% porous CFD result, but has a curve with a lower slope, causing it to overestimate the depth for up to 12 feet and underestimate the depth beyond 12 feet for wider roads.

The vertical distribution of the magnitude of water velocity obtained from the rough surface models on a plane section located at the boundary between the travel lane and the road shoulder is presented in Figure 5-22 for this case. Water velocity in the porous region is the superficial velocity. A negative Z coordinate indicates the porous region and positive Z coordinate corresponds to fluid region. The point of maximum velocity is at the free surface. The profiles include the velocity of air above the free surface, which is not moving except for a boundary layer of flow induced by the motion of the water. Above the free surface, the velocity of air drops back to zero. Both the water surface elevation and the velocity profile change depending on the porosity and depth of the porous region representing the rough surface. The velocity profile in the porous region is significantly different from the fluid region. With increasing porosity, the water depth decreases, and its velocity magnitude increases maintaining the same discharge determined by the rainfall intensity. The smooth surface solution predicts the greatest velocity magnitude close to the surface, out of all models.

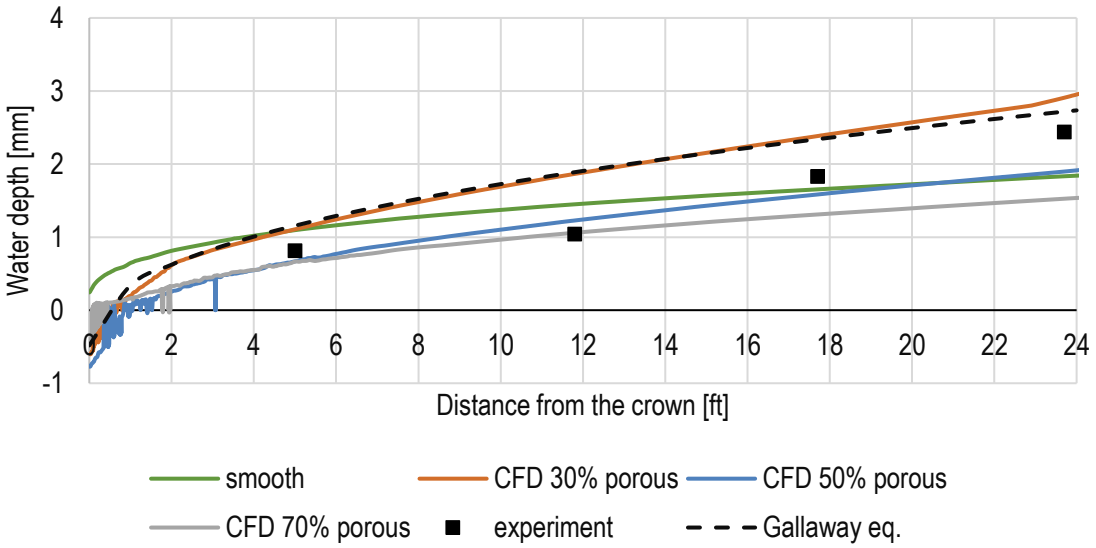

Figure 5-21: Water film thickness on a two-lane wide Surface 4 (T_{XD}=0.5 mm) with cross slope S_X=0.5% at rain intensity R_I=2.21 in/hr

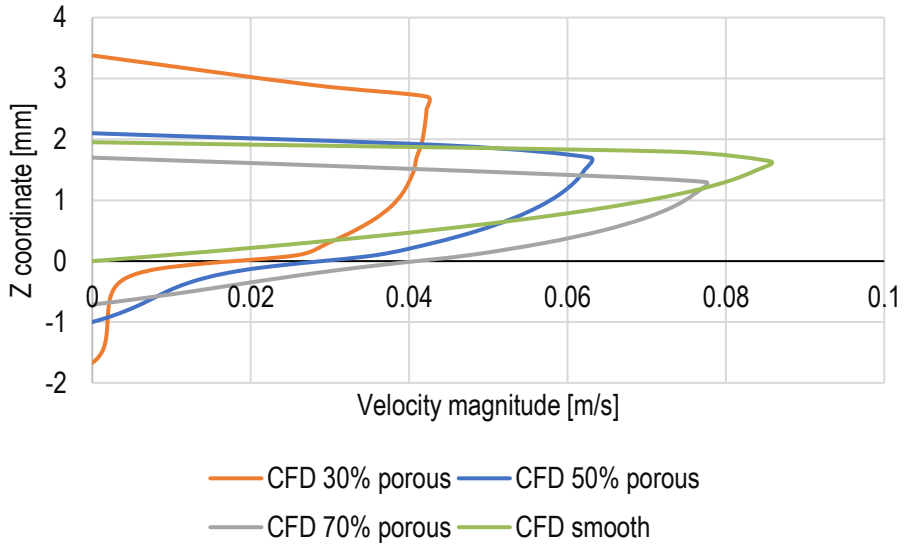

Figure 5-22: Vertical distribution of the magnitude of water velocity on a plane section at a shoulder of a two-lane road

Figure 5-23 shows water depth curves for a road with mean texture depth 0.5 mm and cross-slope 4% at rain intensity 5.5 in/hr. All four measurement points gave a positive reading, which means that tire can come in contact with the water film. The rough surface models with 30% and 50% porosity gave similar results and fall close to the experimental measurements and the Gallaway equation curve. The 70% porous CFD model underestimated the experiment. The curve obtained from the smooth surface model falls close to the rest of the plots, but again has a smaller slope

and underestimates the experiment starting at ~6ft away from the crown, which may lead to an underprediction of the water depth as compared to the Gallaway equation and other CFD models, for multilane roads, especially roads with more than 2 lanes of water draining across them.

Under the assumed conditions, when mean texture depth is equal 0.5 mm, most of the flow occurs in the fluid region (above the texture) and that is where most of the water free surface forms. The water surface has a negative elevation (is below the top of the macrotexture) only within 1 foot to 2 feet away from the crown in the presented examples. The Gallaway et al. experiments showed that the water depth is greater than texture depth in most of the test cases. Only under conditions of low rain intensity combined with high slopes, does it fall into the negative range over a distance up to 2 ft from the crown.

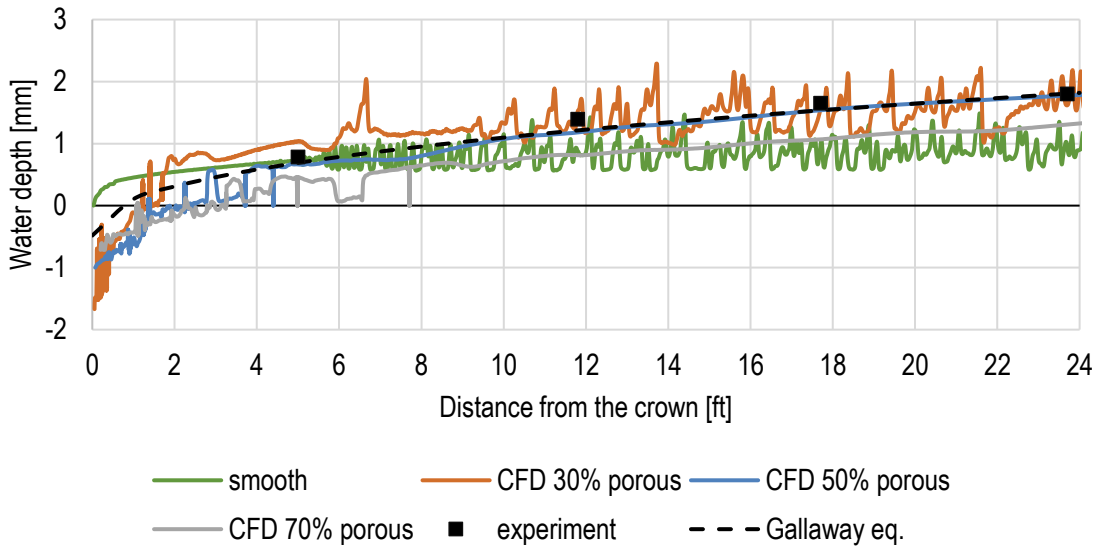

Figure 5-23: Water film thickness on a two-lane wide Surface 4 (T_{XD}=0.5 mm) with cross slope S_X=4%, at rain intensity R_I=5.5 in/hr

Figure 5-24 presents the water depth distribution across the road obtained for Surface 1 (T_{XD}=0.9mm) with cross slope 2% and 6.05 in/hr rain intensity. The experiment has the water film is above the asperities of the macrotexture at least starting 6 feet from the crown. The plots obtained from the rough surface models differ from the measured value by to up to 1 mm in water depth at the shoulder (L=24 ft). The models with 30% and 50% porosity gave a similar fit to the experimental data points. The model with 70% porosity underestimates the experimental measurements. The smooth surface model approximates the water depth well out to nearly 24 ft from the crown, but its slope is smaller and therefore it will underpredict water depth for larger distances.

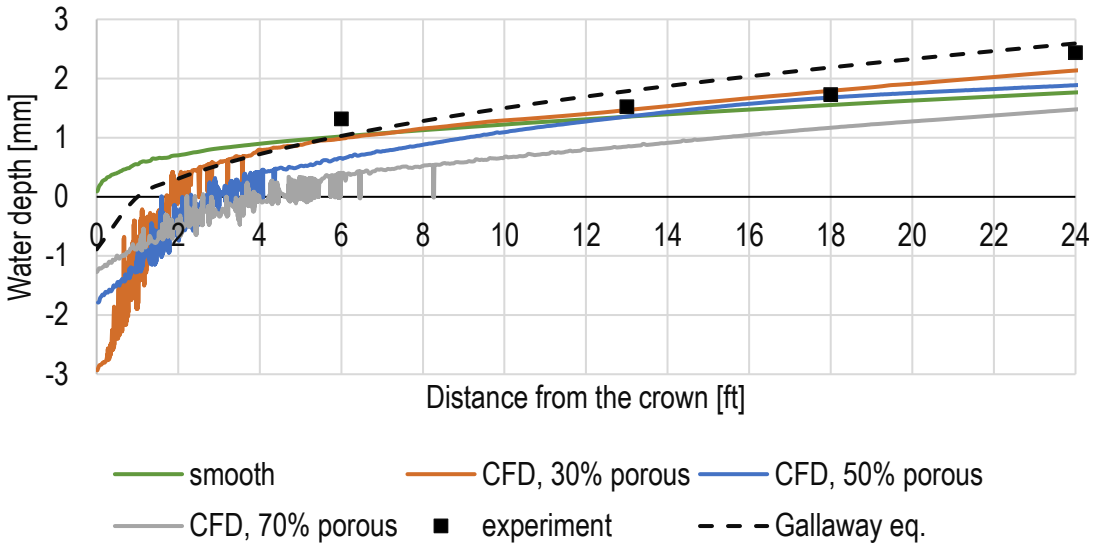

Figure 5-24: Water film thickness on a two-lane wide Surface 1 (T_{XD}=0.9mm) with cross slope S_X=2% at rain intensity R_I=6.05in/hr

As shown in Figure 5-25, for a case with a relatively large cross-slope of 4% and low rain intensity of 0.63 in/hr, the water height predicted by the rough CFD models with 50% and 70% porosity remains mostly below the macrotexture (zero on the vertical axis), the same as the experimental measurement and Gallaway equation curve. The Gallaway equation does not account for the presence of solids taking up space within the texture and therefore the water depth grows from -T_{XD}. The rough road volume grows and consequently so does the porous region depth to match the texture water storage capacity as porosity decreases. Consequently, the water film starts from a lower level at lower porosity but grows faster because there is less void space per unit volume. In this case there may be issues comparing water depths when the k_s is not known, however, the 50% porous case appears to do well after 6 ft. The CFD smooth model overpredicts the water height, but it yields a value of only 0.5 mm at 24 ft, which is conservative, but not excessively with respect to hydroplaning hazard.

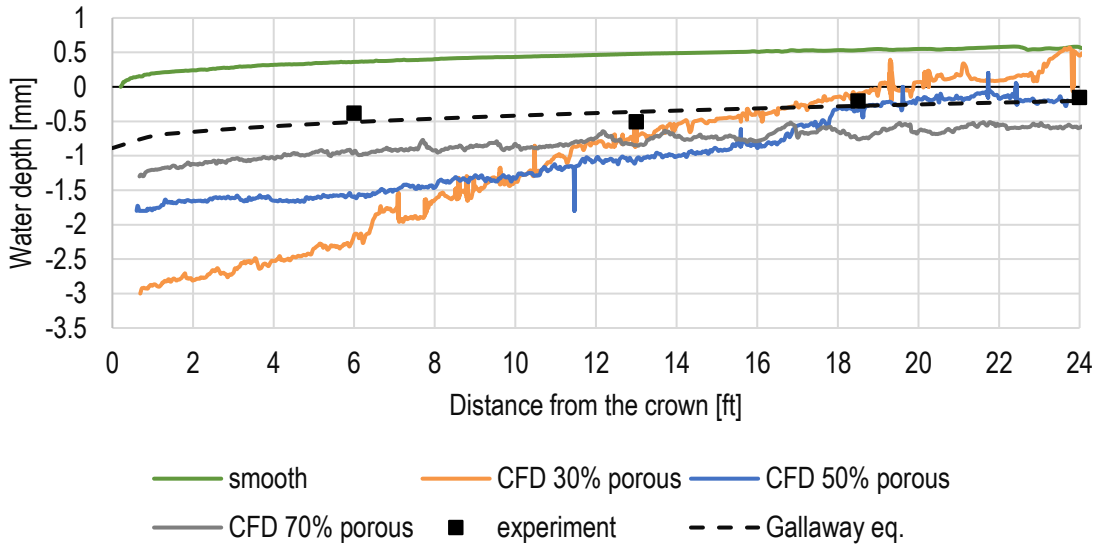

Figure 5-25: Water film thickness on a two-lane wide Surface 1 (T_{XD}=0.9mm) with cross slope S_X=4% at rain intensity R_I=0.63in/hr

The value of porosity of the porous region representing the rough surface has the most influence on the water depth prediction in the case of the models of a pavement with larger texture depth. In this case a significant part of the flow occurs in the porous region (below the tops of the asperities). Gallaway et al. experimental results showed that negative values of water depth prevail and the water free surface rises above the top of the texture depth only for the lowest cross-slope (0.5%) in combination with high rain intensities (above 2 in/hr).

Figure 5-26 presents the results for a surface with mean texture depth 3.6 mm, cross slope 0.5% and rain intensity 2.48 in/hr. The smooth surface model noticeably overestimates the experimental measurements along the width of the road but comes close to the maximum measured water depth 24 feet away from the crown. The rough surface model results fall above or below the experimental data points, depending on the porosity. The model with porosity equal to 30% overestimates slightly the experimental results, and the 50% porous model is very close to the data points that are above the road texture. In that case the measured data has the water film in contact with tires (positive values of water depth) only for the right-hand lane, reaching just under 2 mm at 24 ft. In this case, the Gallaway equation underpredicts the hydroplaning hazard.

Note that with a texture depth of 3.6 mm, typical of asphalt, the road surface has much more capacity to hold water below the plain of a tire than for a texture depth of 0.9 mm that could represent a concrete surface. Under these conditions, risk of hydroplaning is small over two lanes but may become significant over four or six lanes.

Figure 5-27 present the water film for the case of Surface 6 (T_{XD}=3.6mm) with 4% cross slope at rain intensity of 1.98 in/hr. For a relatively large cross-slope of 4%, the water depth is much lower than for 0.5% grade and it is contained within the rough surface. Rough surface models can predict these conditions, whereas the smooth surface model overpredicts the depth.

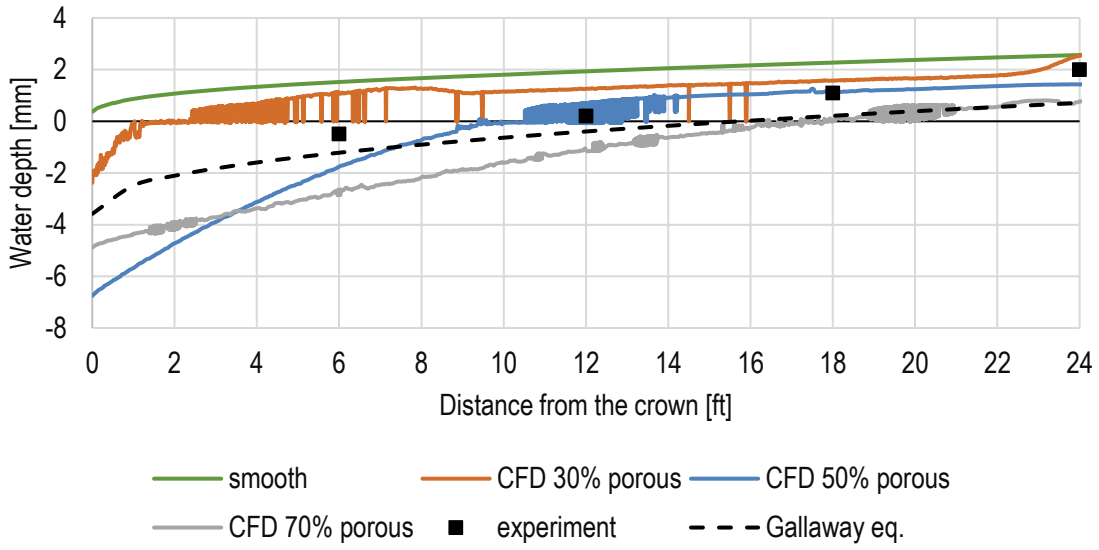

Figure 5-26: Water film thickness on a two-lane wide Surface 6 (T_{XD}=3.6mm) with cross-slope S_X=0.5% at rain intensity R_I=2.48 in/hr

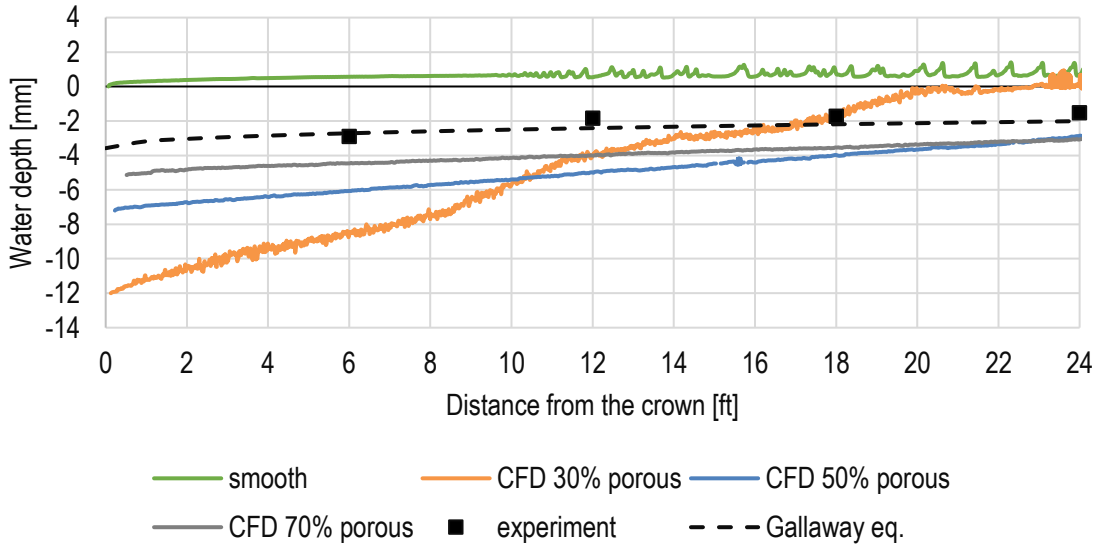

Figure 5-27: Water film thickness on a two-lane wide Surface 6 (T_{XD}=3.6mm) with cross slope S_X=4% at rain intensity R_I=1.98 in/hr

For the above cases, the porous media model of roughness appears to do better that the smooth surface in nearly all cases. The water film thickness appears to increase too slowly with the smooth model when roughness is above the 0.15 mm texture depth used in Part 1 [5]. While the smooth surface model nearly always overpredicts water film thickness for the lane next to the crown due to the zero texture depth, it almost always underpredicts water film thickness in the right lane of the two lane road and this underprediction would become larger on lanes farther to the right due

to the slower growth. This underprediction arises from not accounting for the flow resistance caused by the surface texture. In the porous media cases tested above the model compares very well with both the experimental data and the Gallaway equation for water film depth. The porosity of the Gallaway surfaces was unknown. The 70% porosity cases consistently underestimate the experimental data and therefore 70% appears to be too high. The 30% porosity cases frequently overpredict the experimental data where the water film is positive, at or above the texture. The 50% porosity cases are very close to the experimental data but usually slightly underpredict the data. The porosity that would yield results that best fit the data is therefore likely between 30% and 50% but close to 50%. Because 50% porosity appear to yield best results of the tested porosities, 50% porosity was used in the additional very wide road cases that were tested.

A series of rough surface CFD models using the porous media model were set up and run for a very wide six lane road 72 feet in width. The cases had surface texture depths of 0.5 mm, 0.9 mm, and 3.6 mm, respectively. The cross-slope and rain intensity were selected such that they correspond to cases simulated for two-lane roads and for which Gallaway et al provided experimental measurements up to 24 feet from the road crown. Figures from Figure 5-28 to Figure 5-30 show water film thickness plots for these cases. As mentioned before, close to the crown where the flow occurs within the macrotexture, the smooth surface model overpredicts the film thickness because the film starts growing from zero and not a negative value within the texture layer. Further away from the crown, it gives a close approximation to but slight underprediction of the rough surface model, for the cases when the texture depth is relatively small, up to 0.9 mm. When the texture depth is significantly larger, T_{XD} = 3.6 mm, the smooth surface model gives bigger depth than the rough surface model. The rough surface model overall predicts the experimental measurements well up to the first 24 feet from the crown. When compared to the Gallaway equation curves, both CFD models give a good comparison for the T_{XD} = 0.5 mm. For a surface with T_{XD}=0.9 mm the two CFD models give a similar result, and the Gallaway equation predicts a much deeper water film: the maximum difference is by 1.33 mm at 72 feet away from the crown. For T_{XD}=3.6 mm the Gallaway equation underpredicts the experimental measurements, up to 24 ft, but gives a similar water film thickness at 72 feet, compared to the CFD models.

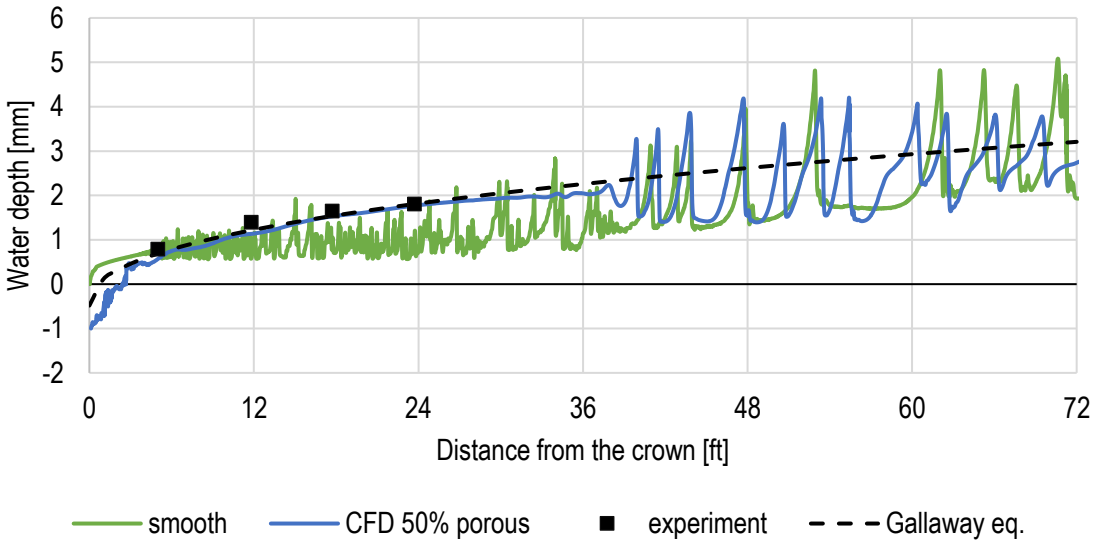

Figure 5-28: Water film thickness on a six-lane (72 ft) wide Surface 4 (T_{XD}=0.5 mm) with cross slope S_X=4%, at rain intensity R_I=5.5 in/hr

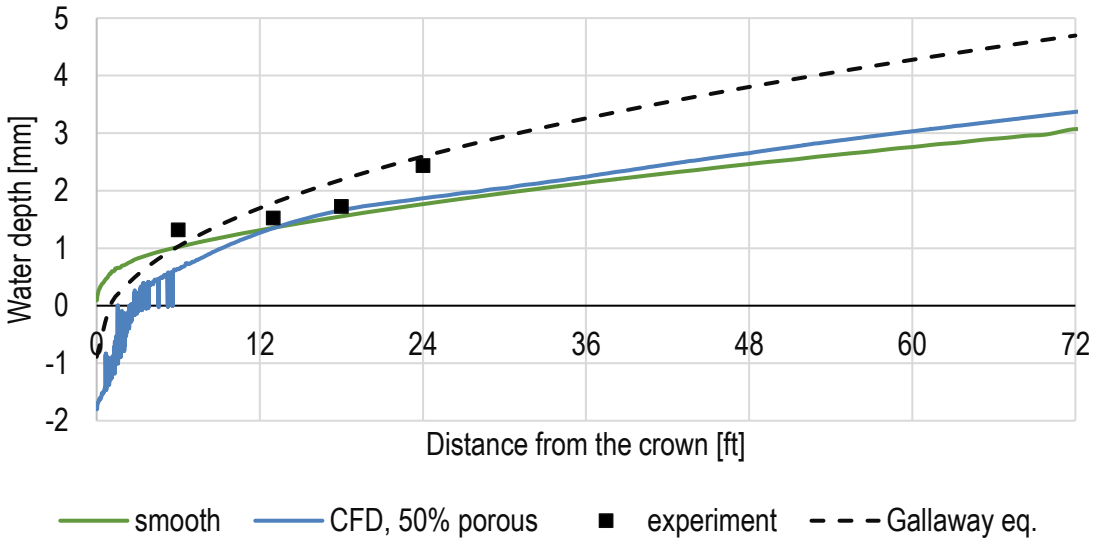

Figure 5-29: Water film thickness on a six-lane (72 ft) wide Surface 1 (T_{XD}=0.9mm) with cross slope S_X=2%, at rain intensity R_I=6.05 in/hr

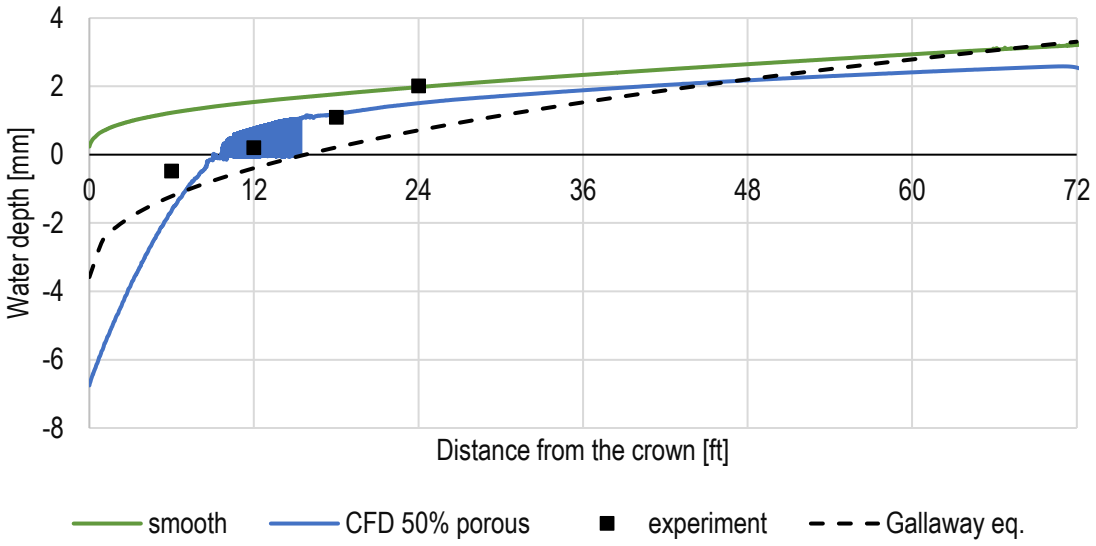

Figure 5-30: Water film thickness on a six-lane (72 ft) wide Surface 6 (T_{XD}=3.6mm) with cross-slope S_X=0.5% at rain intensity R_I=2.48 in/hr

Figures from Figure 5-31 to Figure 5-33 present water film thickness curves for two-lane roads with different surfaces, at a rain intensity 10 in/hr, that is significantly larger than the highest tested in the Gallaway experiments, so in for these cases there is no experimental data result to compare against. In each case, the rough surface model gives greater maximum water film thickness than the smooth surface model, by about 0.5 mm at 24 feet and this difference should increase for lanes farther to the right due to its faster growth rate. The Gallaway equation gives a more conservative prediction. At 24 ft the Gallaway equation overpredicts by 0.6 mm for T_{XD} of 0.6 mm, by 1.3 mm for T_{XD} of 0.9 mm and by 1.9 mm for T_{XD} of 3.6 mm at 24 ft. With that Gallaway curve growing faster than that of the CFD, the Gallaway equation prediction of water depth will exceed that of the CFD by an increasing amount for additional road lanes to the right. The 10 in/hr rain intensity used for these cases is about 1.7 times the largest that Gallaway tested, about 6 in/hr. The dependence on rain intensity in the Gallaway equation, $R_I^{0.59}$, may be too large when extending beyond the original range. Trying to improve the value would require much more result data in the extended range and significant additional work to obtain the data and is beyond the scope of this study.

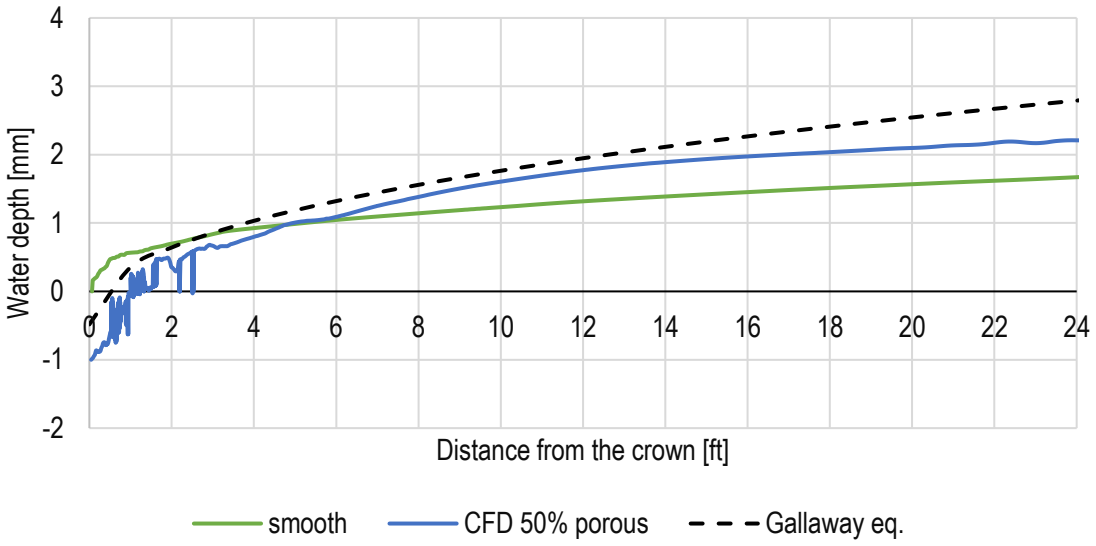

Figure 5-31: Water film thickness on a two-lane wide Surface 4 (T_{XD}=0.5 mm) with cross slope S_X=4% at rain intensity R_I=10 in/hr

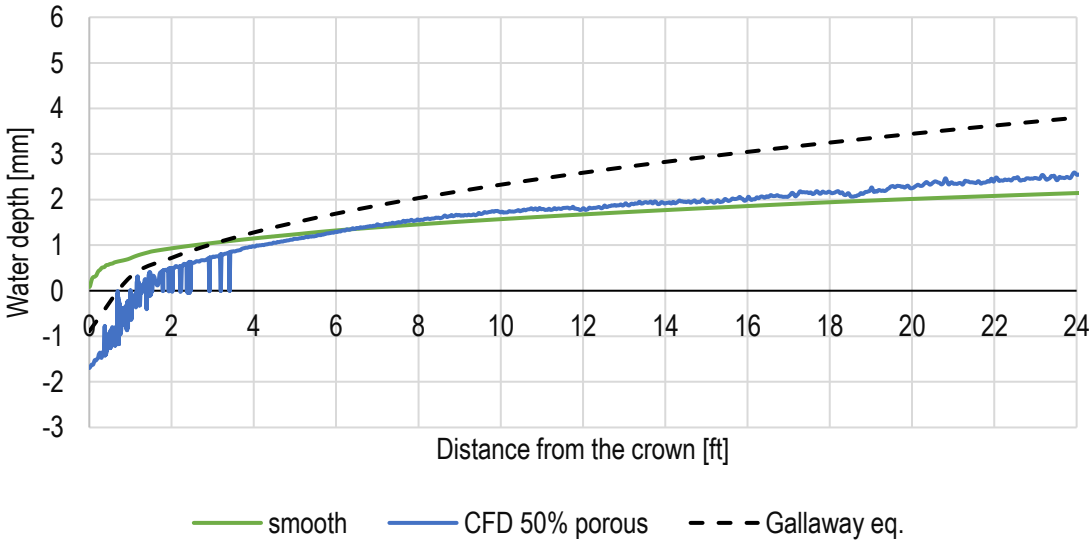

Figure 5-32: Water film thickness on a two-lane wide Surface 1 (T_{XD}=0.9mm) with cross slope S_X=2%, at rain intensity R_I=10.0 in/hr

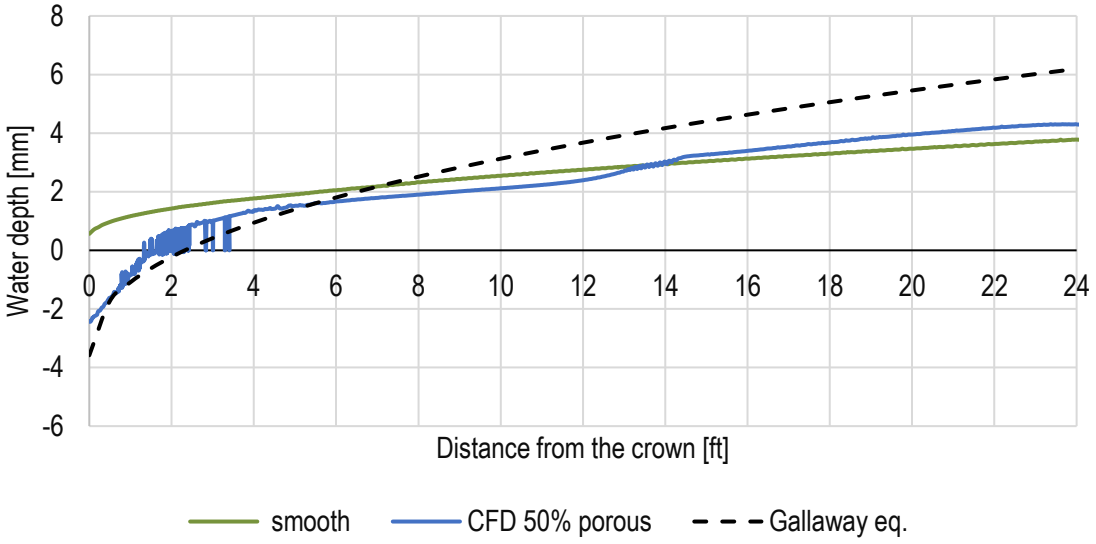

Figure 5-33: Water film thickness on a two-lane wide Surface 6 (T_{XD}=3.6mm) with cross-slope S_X=0.5% at rain intensity R_I=10 in/hr

6. Conclusions

A new approach to the modeling of the effects of surface roughness of water film flow when the roughness height is the same order of magnitude as the water film thickness was developed, tested, and compared to experiment and the empirical equation of Gallaway [3] for predicting water film thickness on roads during rain events.

At the start of this research, the smooth pavement model was the only option for obtaining computational analysis results for water film flow on a wide range of road geometries and conditions rapidly, and it was assumed that it would give results sufficiently accurate for engineering purposes for concrete, but possibly not for asphalt. The study analysis [5] showed that the smooth pavement model yields reasonably accurate results for water film thickness when the roughness height is less than 0.15 mm. Roughness heights this small are not characteristic of most roadways. Three ways to include pavement roughness in the model were investigated: (1) include it as a roughness height, (2) modeling the roughness directly by meshing it out in the domain, and (3) a new approach, modeling the rough surface layer as a porous layer region.

Modeling roughness with the roughness height gives reasonable results in the cases when the water depth is significantly greater than the macrotexture depth. Assigning roughness properties to a wall boundary condition means that the first prism layer above the surface has to be two times the roughness height in thickness. At the same time, the water films thinner than the half-cell size will not be modeled. In many cases considered in this report, and in field conditions, water film thickness forming on a road during a rain event is of the same order of magnitude as the macrotexture depth, therefore the roughness height model is not recommended.

Meshed-out geometry of the pavement gives the most accurate results, as it represents the actual shape of the surface and therefore does not introduce additional modeling errors. Nevertheless,

it is very computationally expensive, as the scale of the macrotexture size (of a few millimeter depth) is at least three orders of magnitude smaller than the size of the section of a road (measured in meters) that has to be taken into account in a simulation to get meaningful results. Only very small models can be built using this approach.

Porous region models provide a practical way to use CFD to analyze water film flow on large sections of roadway as opposed to small patches when the surface texture thickness is comparable to the water film thickness. They occupy a middle ground between the other two approaches, and they were shown to be very useful for modeling rough pavements with texture depth greater than 0.15 mm, which includes most road surfaces. The porous media model requires the aggregate size, texture depth, which is the ratio of texture volume to projected surface area, and the texture porosity. Because porosity was not available from the Gallaway experimental data, three porosities were tested to determine which best matched Gallaway's results. Porous resistance parameters were calculated from the aggregate size and porosity. A porosity of 50% gave a good match with the Gallaway experimental measurements slightly underpredicting them. A porosity of 30% overpredicts water film thickness when it is above the texture. A value between 30% and 50%, but close to 50% is likely to best characterize Gallaway's data set. Additional investigation may yield better values for the surface texture porosity for various road surface types. The surface texture porosity may be obtained by direct measurement from pavement samples.

The porous region models represent the water film thickness on rough surfaces better than the smooth surface models. The growth of the water film from the bottom of the macro texture below where a tire would sit at the top of the asperities is included within the model. The resistance to flow within the porous layer generated by the macrotexture appears to be well captured, and greatly reduces the velocity of film from the open flow region above. That resistance to flow in the porous layer is propagated by shear stress across the interface between the porous region and fluid above. The resulting flow resistance on the water film above macrotexture yields a film growth rate that appears to match very well with both experimental data and the Gallaway equation for water film thickness when the rain intensity is within the range tested by Gallaway up to about 6 in/hr.

The Gallaway experiments and equation for water film thickness only extended to 2 lanes (24 ft). The Gallaway equation appears to be good out to 6 lanes (72 ft) for predicting water film thickness up to rain intensities that are within the range of those tested, about 6 in/hr. At 10 in/hr the Gallaway equation overpredicts the CFD results by a fair amount. More investigation is recommended before applying the Gallaway equation at rain intensities greater than 6 in/hr.

7. Acknowledgements

The funding for this project came from the Hydraulics Research Program at the Turner-Fairbank Highway Research Center, through Interagency Agreement Number DTFH61-14-X-300002 between DOT and DOE, and the work was performed under DOE's contract with UChicago Argonne, LLC, contract no. DE-AC02-06-CH11357.

8. References

[1] Simcenter STAR-CCM+ Documentation, last accessed July 2020, https://documentation.thesteveportal.plm.automation.siemens.com/starccmplus_latest_en/index.html?param=kvkJX&authLoc=https://thesteveportal.plm.automation.siemens.com/AuthoriseRedirect

[2] Gallaway B. M., Epps J. A., Tomita H., Effects of Pavement Surface Characteristics and Textures on Skid Resistance, Texas Transportation Institute Research Report 138-4, 1971

[3] Gallaway B., Schiller R., Rose J., The Effects of Rainfall Intensity, Pavement Cross Slope, Surface Texture, and Drainage Length on Pavement Water Depths, Texas Transportation Institute Research Report 138-5, 1971

[4] Gallaway, B. M. et al., Pavement and Geometric Design Criteria for Minimizing Hydroplaning, FHWA RD-79-31, 1979

[5] Lottes S.A., Sitek M.A., Sinha N., Computational Analysis of Water Film Thickness During Rain Events for Assessing Hydroplaning Risk. Part 1. Nearly Smooth Road Surfaces, ANL-20/36, July 2020

[6] McGahey C., Samuels P.G., River roughness-the integration of diverse knowledge, River Flow 2004 – Greco, Carravetta & Della Morte (eds.), Taylor& Francis Group, London, ISBN 90-5809-658-0

Nuclear Science and Engineering Division
Argonne National Laboratory
9700 South Cass Avenue, Bldg. 208
Argonne, IL 60439-4815

www.anl.gov

Argonne National Laboratory is a U.S. Department of Energy laboratory managed by UChicago Argonne, LLC